Transverse Momentum Dependent Helicity Distributions

26th International Symposium on Spin Physics (SPIN2025)
September 23th, 2025

Ke Yang (杨科)

Institute of Frontier and Interdisciplinary science, Shandong University, Qingdao 266237, China

In collaboration with: Tianbo Liu, Bo-Qiang Ma, Peng Sun, Yuxiang Zhao

Transverse Nucleon Tomography Collaboration

Phys.Rev.Lett. 134 (2025) 12, 121902

SHANDONG UNIVERSITY

26th International Symposium on Spin Physics
A Century of Spin

Introduction

Protons and neutrons are the primary constituents of visible matter in the universe.

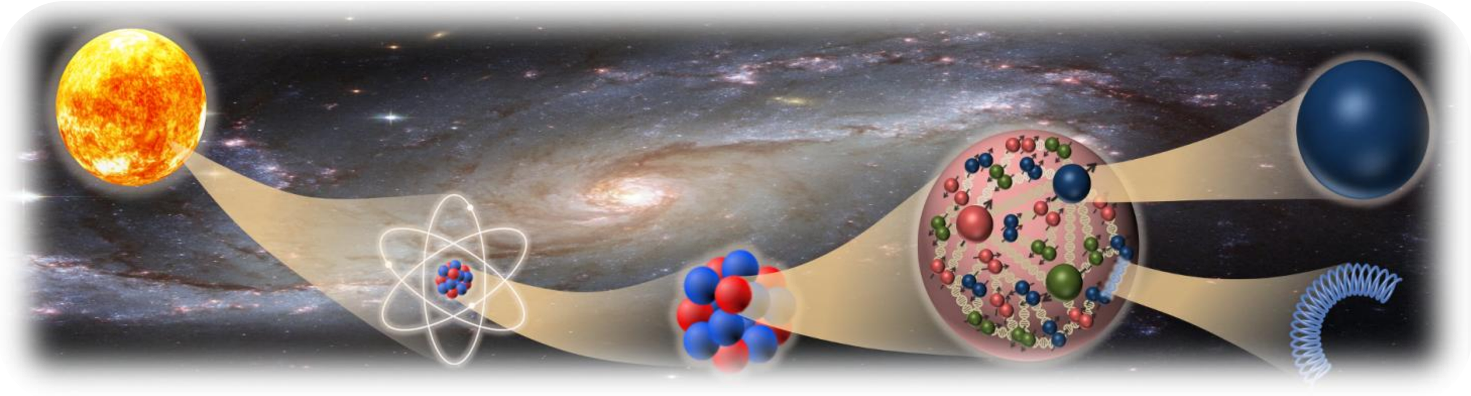

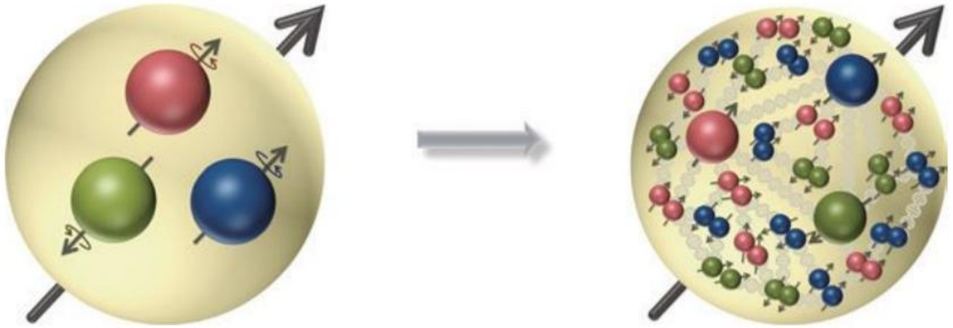

Mass

Spin

SHANDONG UNIVERSITY, QINGDAO

Proton Spin Structure in Naïve Quark Model

Quark model:

M. Gell-Mann, Phys. Lett. 8, 214 (1964);
G. Zweig, CERN Report No. TH-401 (1964).

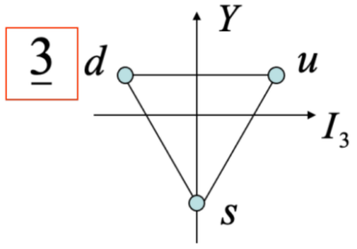

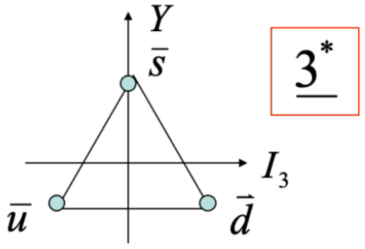

Color structure:

$\underline{3} \times \underline{3}^* = \underline{8} + \boxed{\underline{1}}$ ⟶ Ordinary mesons

$\underline{3} \times \underline{3} \times \underline{3} = \underline{10} + \underline{8} + \underline{8} + \boxed{\underline{1}}$ ⟶ Ordinary baryons

Proton wave function in spin flavor space

$$|p_\uparrow\rangle = \frac{1}{\sqrt{18}} [2\,|u_\uparrow d_\downarrow u_\uparrow\rangle + 2\,|u_\uparrow u_\uparrow d_\downarrow\rangle + 2\,|d_\downarrow u_\uparrow u_\uparrow\rangle - |u_\uparrow u_\downarrow d_\uparrow\rangle$$
$$- |u_\uparrow d_\uparrow u_\downarrow\rangle - |u_\downarrow d_\uparrow u_\uparrow\rangle - |d_\uparrow u_\downarrow u_\uparrow\rangle - |d_\uparrow u_\uparrow u_\downarrow\rangle - |u_\downarrow u_\uparrow d_\uparrow\rangle] \,.$$

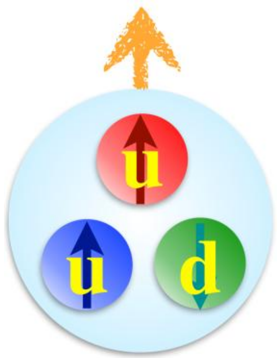

$$\Delta u = u_\uparrow - u_\downarrow = \frac{4}{3} \qquad \Delta d = d_\uparrow - d_\downarrow = -\frac{1}{3}$$

The spin of the proton comes entirely from the spin of the quarks!

Proton Spin Structure

J. Ashman *et al.* (EMC) PLB 206, 364 (1988).

J. Ashman *et al.* (EMC) NP B328, 1 (1989).

Experimental data:

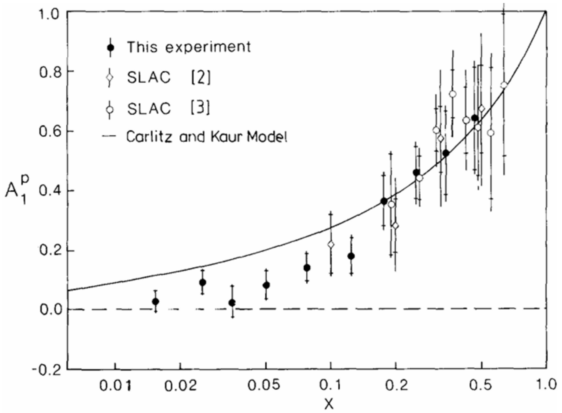

$$\Delta\Sigma = 0.114 \pm 0.012 \pm 0.026.$$

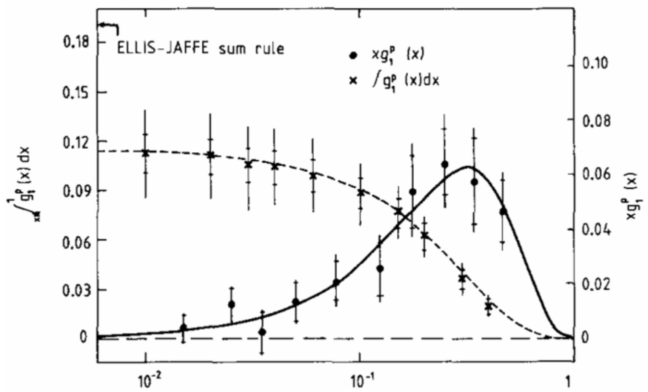

$$\Delta\Sigma = 0.126 \pm 0.010 \pm 0.015.$$

Global analysis:

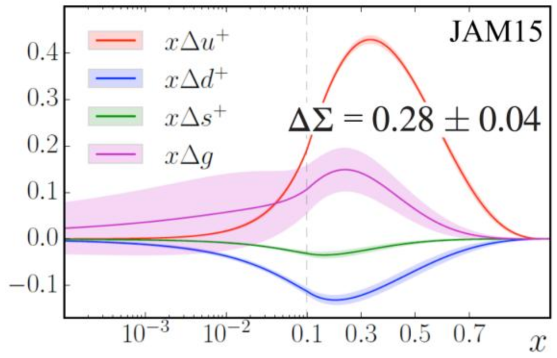

JAM Collaboration, PR D 93, 074005 (2016).

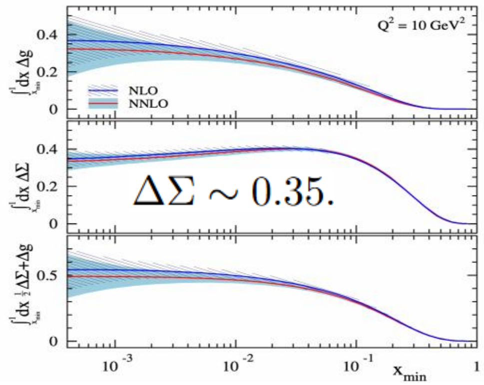

I. Borsa *et al.* Phys.Rev.Lett. 133, 151901 (2024).

Lattice calculation:

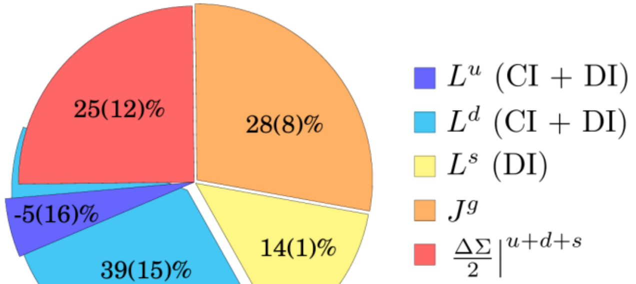

$$\Delta\Sigma \sim 0.25 \pm 12.$$

χQCD Collaboration, PR D 91, 014505 (2015).

Proton Spin Structure

Spin decomposition:

$$J = \frac{1}{2}\Delta\Sigma + L_q + \Delta G + L_g,$$

R. Jaffe and A. Manohar, Nucl.Phys. B337 (1990) 509.

$$\Delta\Sigma = \Delta u + \Delta d \sim 0.3$$

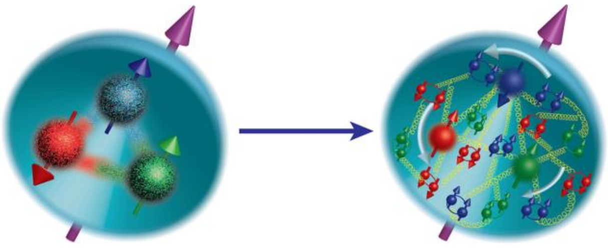

Melosh-Wigner rotation: nucleon in its rest frame V.S. in infinite momentum frame

E. P. Wigner, Annals Math. 40, 149 (1939);
H. J. Melosh, Phys. Rev. D 9, 1095 (1974).

spin state:

$$\chi_T^{\uparrow} = w\left[\left(k^+ + m\right)\chi_F^{\uparrow} - \left(k^1 + ik^2\right)\chi_F^{\downarrow}\right] \qquad k^+ = k^0 + k^3$$

$$\chi_T^{\downarrow} = w\left[\left(k^+ + m\right)\chi_F^{\downarrow} + \left(k^1 - ik^2\right)\chi_F^{\uparrow}\right] \qquad w = \left[2k^+\left(k^0 + m\right)\right]^{-1/2}$$

Quark polarization state: $\Delta q = \int \mathrm{d}^3\mathbf{k}\mathscr{M}\left[q^{\uparrow}(k) - q^{\downarrow}(k)\right] \qquad \mathscr{M} = \dfrac{\left(k^+ + m\right)^2 - k_T^2}{2k^+\left(k^0 + m\right)}$

B.-Q. Ma, J. Phys. G 17, L53-L58 (1991);B.-Q. Ma, Z.Phys. C 58, 479 (1993).

The Melosh-Wigner rotation predicts decreasing polarization with transverse momentum, and this prediction should be tested by data.

Transverse Mometum Dependent PDFs

Definition:

$$\Phi_{ij}(x,p_T) = \int \frac{d\xi^- d^2\boldsymbol{\xi}_T}{(2\pi)^3}\, e^{ip\cdot\xi}\, \langle P|\bar{\psi}_j(0)\,\mathcal{U}^{n-}_{(0,+\infty)}\,\mathcal{U}^{n-}_{(+\infty,\xi)}\,\psi_i(\xi)|P\rangle\Big|_{\xi^+=0}$$

		Quark Polarization		
		Un-Polarized (U)	Longitudinally Polarized (L)	Transversely Polarized (T)
Nucleon Polarization	U	f_1 = Unpolarized		$h_1^\perp$ = − Boer-Mulders
	L		g_1 = − Helicity	$h_{1L}^\perp$ = − Worm-gear
	T	$f_{1T}^\perp$ = − Sivers	$g_{1T}^\perp$ = − Worm-gear	h_1 = − Transversity $h_{1T}^\perp$ = − Pretzelosity

R. Boussarie, *et al.* TMD Handbook, arXiv:2304.03302

Structure functions of SIDIS

SIDIS process: $\ell(l) + N(P) \to \ell(l') + h(P_h) + X,$

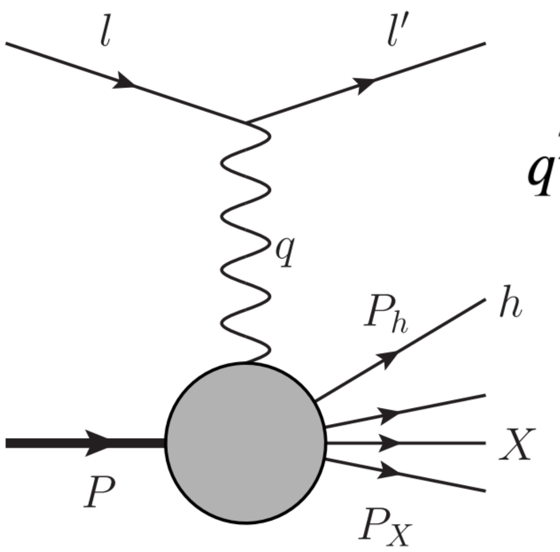

$q^2 = -Q^2$

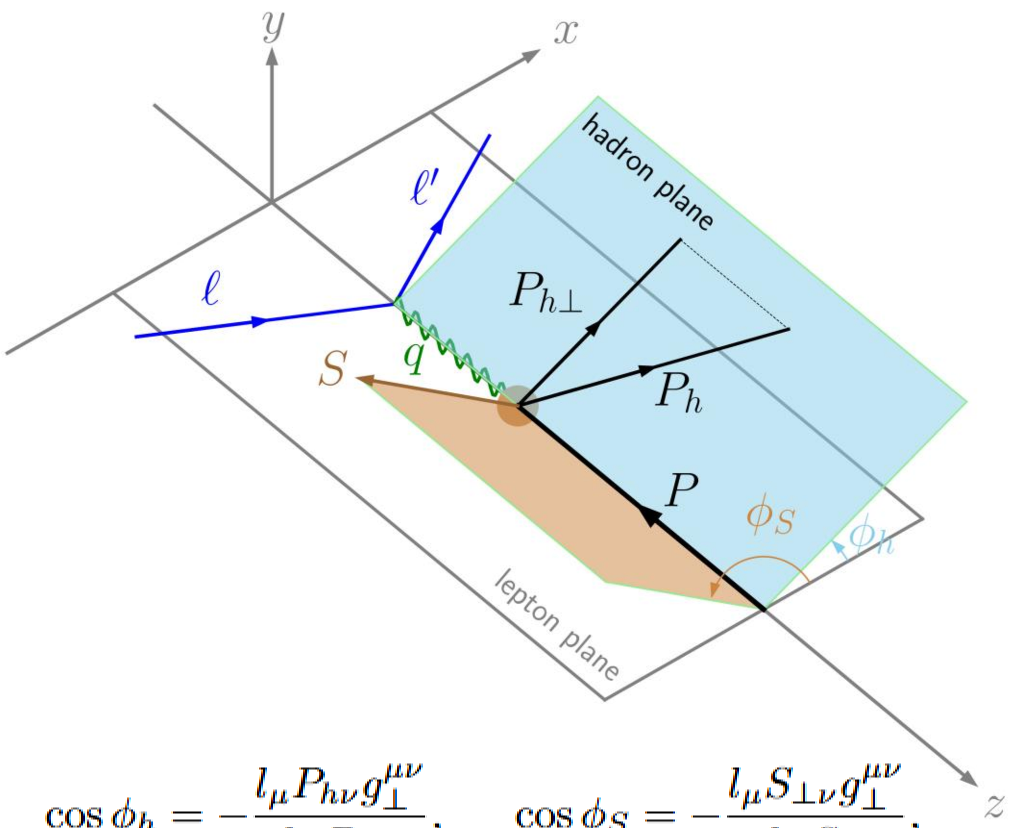

$$x = \frac{Q^2}{2P\cdot q} \quad y = \frac{P\cdot q}{P\cdot l} \quad z = \frac{P\cdot P_h}{P\cdot q}$$

$$\gamma = \frac{2M_N x}{Q} \quad \varepsilon = \frac{1-y-\frac{1}{4}\gamma^2 y^2}{1-y+\frac{1}{2}y^2+\frac{1}{4}\gamma^2 y^2}$$

$$\cos\phi_h = -\frac{l_\mu P_{h\nu} g_\perp^{\mu\nu}}{l_\perp P_{hT}}, \qquad \cos\phi_S = -\frac{l_\mu S_{\perp\nu} g_\perp^{\mu\nu}}{l_\perp S_\perp},$$

$$\sin\phi_h = -\frac{l_\mu P_{h\nu} \epsilon_\perp^{\mu\nu}}{l_\perp P_{hT}}, \qquad \sin\phi_S = -\frac{l_\mu S_{\perp\nu} \epsilon_\perp^{\mu\nu}}{l_\perp S_\perp},$$

Structure functions of SIDIS

SIDIS process:

$$\ell(l) + N(P) \to \ell(l') + h(P_h) + X,$$

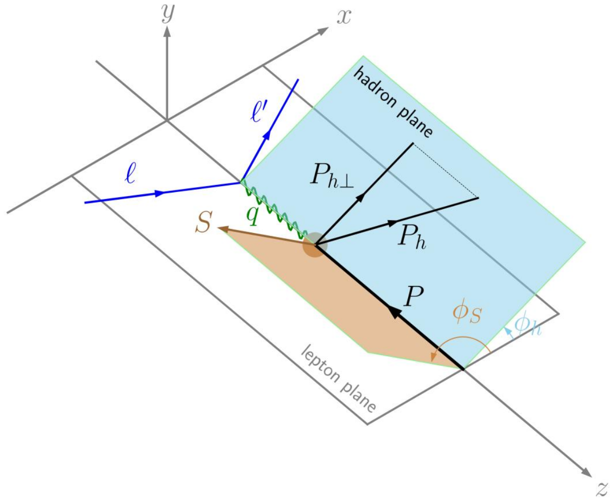

$$F^{m}_{AB,C}(x,z,P_{hT}^2,Q^2) \sim f \otimes D$$

A: lepton polarization

B: nucleon polarization

C: virtual photon polarization

m: angular modulation

$$\frac{\mathrm{d}\sigma}{\mathrm{d}x_B\ \mathrm{d}y\ \mathrm{d}z\ \mathrm{d}P_{hT}^2\ \mathrm{d}\phi_h\ \mathrm{d}\phi_S}$$

$$= \frac{\alpha^2}{x_B y Q^2}\frac{y^2}{2(1-\epsilon)}\left(1+\frac{\gamma^2}{2x_B}\right)$$

$$\times \Big\{ F_{UU,T} + \epsilon F_{UU,L} + \sqrt{2\epsilon(1+\epsilon)} F_{UU}^{\cos\phi_h} \cos\phi_h + \epsilon F_{UU}^{\cos 2\phi_h} \cos 2\phi_h + \lambda_e \sqrt{2\epsilon(1-\epsilon)} F_{LU}^{\sin\phi_h} \sin\phi_h$$

$$+ S_L \left[\sqrt{2\epsilon(1+\epsilon)} F_{UL}^{\sin\phi_h} \sin\phi_h + \epsilon F_{UL}^{\sin 2\phi_h} \sin 2\phi_h \right] + \lambda_e S_L \left[\sqrt{1-\epsilon^2} F_{LL} + \sqrt{2\epsilon(1-\epsilon)} F_{LL}^{\cos\phi_h} \cos\phi_h \right]$$

$$+ S_T \Big[\left(F_{UT,T}^{\sin(\phi_h-\phi_S)} + \epsilon F_{UT,L}^{\sin(\phi_h-\phi_S)} \right) \sin(\phi_h-\phi_S) + \epsilon F_{UT}^{\sin(\phi_h+\phi_S)} \sin(\phi_h+\phi_S)$$

$$+ \epsilon F_{UT}^{\sin(3\phi_h-\phi_S)} \sin(3\phi_h-\phi_S) + \sqrt{2\epsilon(1+\epsilon)} F_{UT}^{\sin\phi_S} \sin\phi_S + \sqrt{2\epsilon(1+\epsilon)} F_{UT}^{\sin(2\phi_h-\phi_S)} \sin(2\phi_h-\phi_S) \Big]$$

$$+ \lambda_e S_T \Big[\sqrt{1-\epsilon^2} F_{LT}^{\cos(\phi_h-\phi_S)} \cos(\phi_h-\phi_S)$$

$$+ \sqrt{2\epsilon(1-\epsilon)} F_{LT}^{\cos\phi_S} \cos\phi_S + \sqrt{2\epsilon(1-\epsilon)} F_{LT}^{\cos(2\phi_h-\phi_S)} \cos(2\phi_h-\phi_S) \Big] \Big\}$$

18 structure functions

Double Spin Asymmetry

Double spin asymmetry:

$$A_{LL}(\phi_h) = \frac{1}{|S_\perp||\lambda_e|}\frac{[\mathrm{d}\sigma_{LL}(+,+) - \mathrm{d}\sigma_{LL}(-,+)]}{\mathrm{d}\sigma_{LL}(+,+) + \mathrm{d}\sigma_{LL}(-,+)}$$
$$= \sqrt{1-\varepsilon^2}\frac{F_{LL}}{F_{UU,T}} + \sqrt{2\varepsilon(1-\varepsilon)}\cos\phi_h \frac{F_{LL}^{\cos\phi_h}}{F_{UU,T}}.$$

$$\Rightarrow$$

$$A_{LL} = \sqrt{1-\varepsilon^2}\frac{F_{LL}}{F_{UU,T}}$$
$$A_{LL}^{\cos\phi_h} = \sqrt{2\varepsilon(1-\varepsilon)}\frac{F_{LL}^{\cos\phi_h}}{F_{UU,T}}$$

Structure functions:

$$F_{UU,T} = \mathcal{C}[f_1 D_1],$$
$$F_{LL} = \mathcal{C}[g_{1L} D_1],$$
$$F_{LL}^{\cos\phi} = \frac{2M}{Q}\mathcal{C}\left[\frac{\hat{\boldsymbol{h}}\cdot\boldsymbol{p}_T}{M_h}\left(x e_L H_1^\perp - \frac{M_h}{M} g_{1L}\frac{\tilde{D}^\perp}{z}\right) - \frac{\hat{\boldsymbol{h}}\cdot\boldsymbol{k}_T}{M}\left(x g_L^\perp D_1 + \frac{M_h}{M} h_{1L}^\perp \frac{\tilde{E}}{z}\right)\right]$$
$$\approx -\frac{2M}{Q}\mathcal{C}\left[\frac{\hat{\boldsymbol{h}}\cdot\boldsymbol{k}_T}{M}(g_{1L}D_1)\right]$$
$$x g_L^\perp = x\tilde{g}_L^\perp + g_{1L} + \frac{m}{M_N}h_{1L}^\perp \approx g_{1L}.$$

$$\Rightarrow$$

TMD PDF:

$f_1(x, k_T)$

$g_{1L}(x, k_T)$

TMD FF:

$D_1(x, p_T)$

Energy Evolution

Evolution equation:

$$\mu\frac{\mathrm{d}\mathcal{F}(x,b_T;\mu,\zeta)}{\mathrm{d}\mu}=\gamma_\mu(\mu,\zeta)\mathcal{F}(x,b_T;\mu,\zeta)$$

$$\zeta\frac{\mathrm{d}\mathcal{F}(x,b_T;\mu,\zeta)}{\mathrm{d}\zeta}=-\mathcal{D}(\mu,b_T)\mathcal{F}(x,b_T;\mu,\zeta)$$

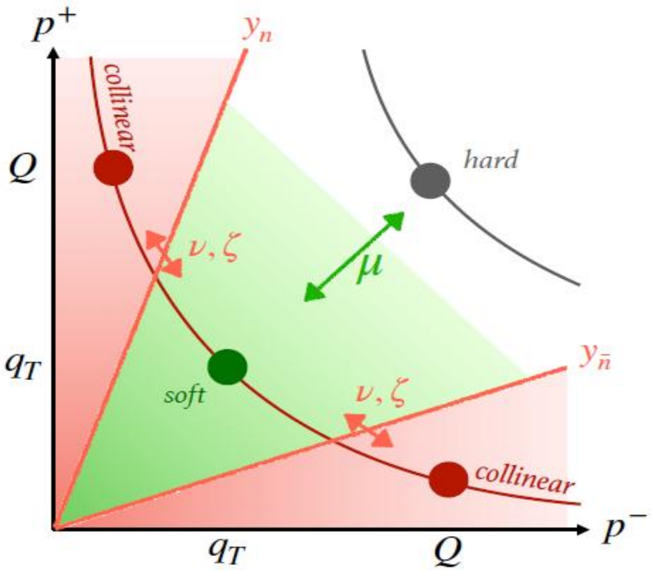

R. Boussarie, *et al.* TMD Handbook, arXiv:2304.03302

ζ-prescription evolution path:

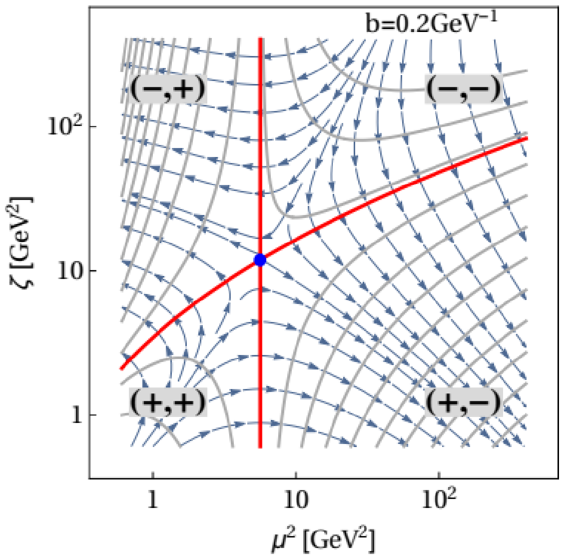

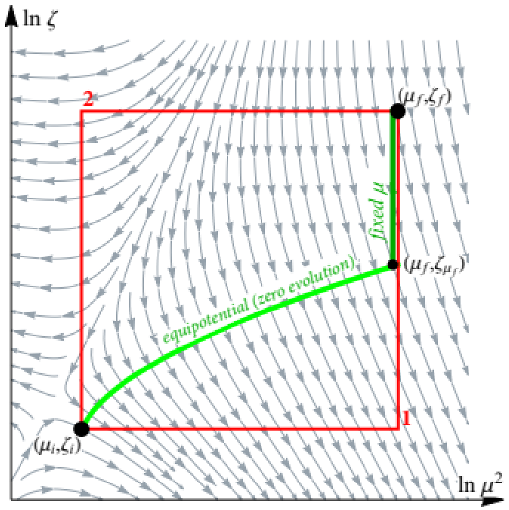

$$R[b_T;(\mu_i,\zeta_i)\to(Q,Q^2)]\;=\;\left[\frac{Q^2}{\zeta_\mu(Q,b_T)}\right]^{-\mathcal{D}(Q,b_T)}$$

I. Scimemi and A. Vladimirov, J. High Energy Phys. 06 (2020) 137
R. Boussarie, *et al.* TMD Handbook, arXiv:2304.03302

Parametrization

Unpolarized TMDs: **SV19 Model**

I. Scimemi and A. Vladimirov, J. High Energy Phys. 06 (2020) 137

Optimal TMD PDF&FF at saddle point

Collinear unpolarized PDF input, NNPDF3.1

$$f_{1;f\leftarrow h}(x,b_T)=\sum_{f'}\int_x^1\frac{dy}{y}C_{f\leftarrow f'}(y,b_T,\mu_{\mathrm{OPE}})\,f_{1,f'\leftarrow h}\left(\frac{x}{y},\mu_{\mathrm{OPE}}\right)f_{\mathrm{NP}}(x,b_T),$$

$$D_{1;f\rightarrow h}(z,b_T)=\frac{1}{z^2}\sum_{f'}\int_z^1\frac{dy}{y}y^2\mathbb{C}_{f\leftarrow f'}(y,b_T,\mu_{\mathrm{OPE}})\,d_{1,f'\rightarrow h}\left(\frac{z}{y},\mu_{\mathrm{OPE}}\right)D_{\mathrm{NP}}(z,b_T),$$

Collinear unpolarized FF input, DSS

Parametrization for Non-perturbative functions:

$$f_{\mathrm{NP}}(x,b_T)=\exp\left(-\frac{\lambda_1(1-x)+\lambda_2x+x(1-x)\lambda_5}{\sqrt{1+\lambda_3x^{\lambda_4}b_T^2}}b_T^2\right),$$

$$D_{\mathrm{NP}}(x,b_T)=\exp\left(-\frac{\eta_1z+\eta_2(1-z)b_T^2}{\sqrt{1+\eta_3(b_T/z)^2}}\cdot\frac{b_T^2}{z^2}\right)\left(1+\eta_4\frac{b_T^2}{z^2}\right).$$

Operator product expand energy scale:

$$\mu_{\mathrm{OPE}}^{\mathrm{PDF}}=\frac{2e^{-\gamma_E}}{b_T}+2\mathrm{GeV},$$

$$\mu_{\mathrm{OPE}}^{\mathrm{FF}}=\frac{2e^{-\gamma_E}z}{b_T}+2\mathrm{GeV},$$

Unpolarized TMDs at final energy scale:

$$f_1(x,b_T;Q,Q^2)=R(b_T,Q)\,f_1(x,b_T),\qquad D_1(x,b_T;Q,Q^2)=R(b_T,Q)\,D_1(x,b_T)$$

Parametrization

Collinear helicity distribution input, NNPDFpol1.1

TMD helicity distribution:

Parametrization for TMD helicity distribution at saddle point:

$$g_{1L}^{f}(x, b_T) = \sum_{f'} \int_x^1 \frac{d\xi}{\xi} \Delta C_{f\leftarrow f'}(\xi, b_T, \mu_{\mathrm{OPE}}) \times g_{1L}^{f'}\left(\frac{x}{\xi}, \mu_{\mathrm{OPE}}\right) g_{\mathrm{NP}}(x, b_T).$$

Modified collinear helicity distribution input, left $\boldsymbol{\alpha}, \boldsymbol{\beta}, \boldsymbol{\varepsilon}$ as free parameters to be fitted:

$$g_{1L}^{f}(x, \mu_{\mathrm{OPE}}) = N_f \frac{(1-x)^{\alpha_f} x^{\beta_f} (1+\varepsilon_f x)}{n(\alpha_f, \beta_f, \varepsilon_f)} g_1^f(x, \mu_{\mathrm{OPE}})$$

The x −shape modification can be removed by setting $\boldsymbol{\alpha}, \boldsymbol{\beta}, \boldsymbol{\varepsilon} = 0$.

The $\boldsymbol{n}(\boldsymbol{\alpha}, \boldsymbol{\beta}, \boldsymbol{\varepsilon})$ factor is introduced to the correlation between normalization and the shape.

$$g_{\mathrm{NP}}(x, b_T) = \exp\left[-\frac{\lambda_1(1-x) + \lambda_2 x + x(1-x)\lambda_5}{\sqrt{1+\lambda_3 x^{\lambda_4} b_T^2}} b_T^2\right]$$

We take the same form of non-perturbative function as SV19 model takes for $\boldsymbol{f_1}$.

TMD helicity distribution at final energy scale:

$$g_{1L}(x, b_T; Q, Q^2) = R(b_T, Q)\, g_{1L}(x, b_T)$$

World data

TABLE VI. World SIDIS data that reported by HERMES and CLAS, and figures in parenthesis represent numbers of data points satisfy $\delta < 0.5$. $\delta = \frac{P_h}{zQ}$

Data set	Run	Hadron beam	Lepton beam	point number	Process	Measurement
HERMES	1996-2000	H_2	27.6 GeV $e^\pm$	80,30(42,10)	$e^\pm p \to e^\pm \pi^+ X$	A_{LL},$A_{LL}^{\cos\phi}$
HERMES	1996-2000	H_2	27.6 GeV $e^\pm$	80,30(42,11)	$e^\pm p \to e^\pm \pi^- X$	A_{LL},$A_{LL}^{\cos\phi}$
HERMES	1996-2000	D_2	27.6 GeV $e^\pm$	80,30(41,10)	$e^\pm d \to e^\pm \pi^+ X$	A_{LL},$A_{LL}^{\cos\phi}$
HERMES	1996-2000	D_2	27.6 GeV $e^\pm$	80,30(40,9)	$e^\pm d \to e^\pm \pi^- X$	A_{LL},$A_{LL}^{\cos\phi}$
HERMES	1996-2000	D_2	27.6 GeV $e^\pm$	79,30(40,10)	$e^\pm d \to e^\pm K^+ X$	A_{LL},$A_{LL}^{\cos\phi}$
HERMES	1996-2000	D_2	27.6 GeV $e^\pm$	80,30(39,9)	$e^\pm d \to e^\pm K^- X$	A_{LL},$A_{LL}^{\cos\phi}$
CLAS	2009	$^{14}NH_3$	6 GeV e^-	21,21(9,9)	$e^- p \to e^- \pi^0 X$	A_{LL},$A_{LL}^{\cos\phi}$
Total				498,201(253,69)		A_{LL},$A_{LL}^{\cos\phi}$

HERMES, Phys. Rev. D 99, 112001 (2019),
CLAS, Phys. Lett. B 782, 662 (2018).

$$A_{LL}(\phi_h) = A_{LL} + \cos\phi_h A_{LL}^{\cos\phi_h}$$

Fit Procedure

World data fit:

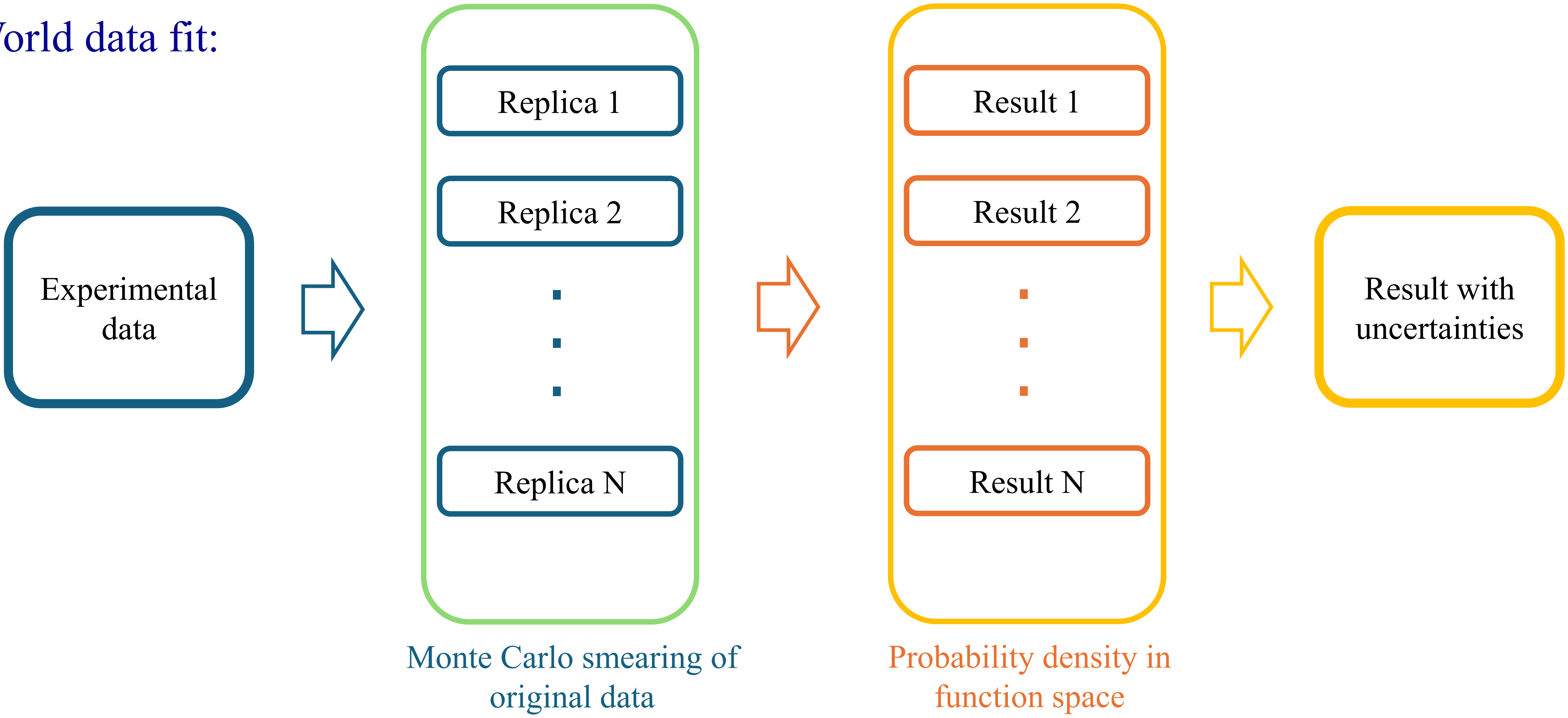

Results

Result of 3D helicity distributions

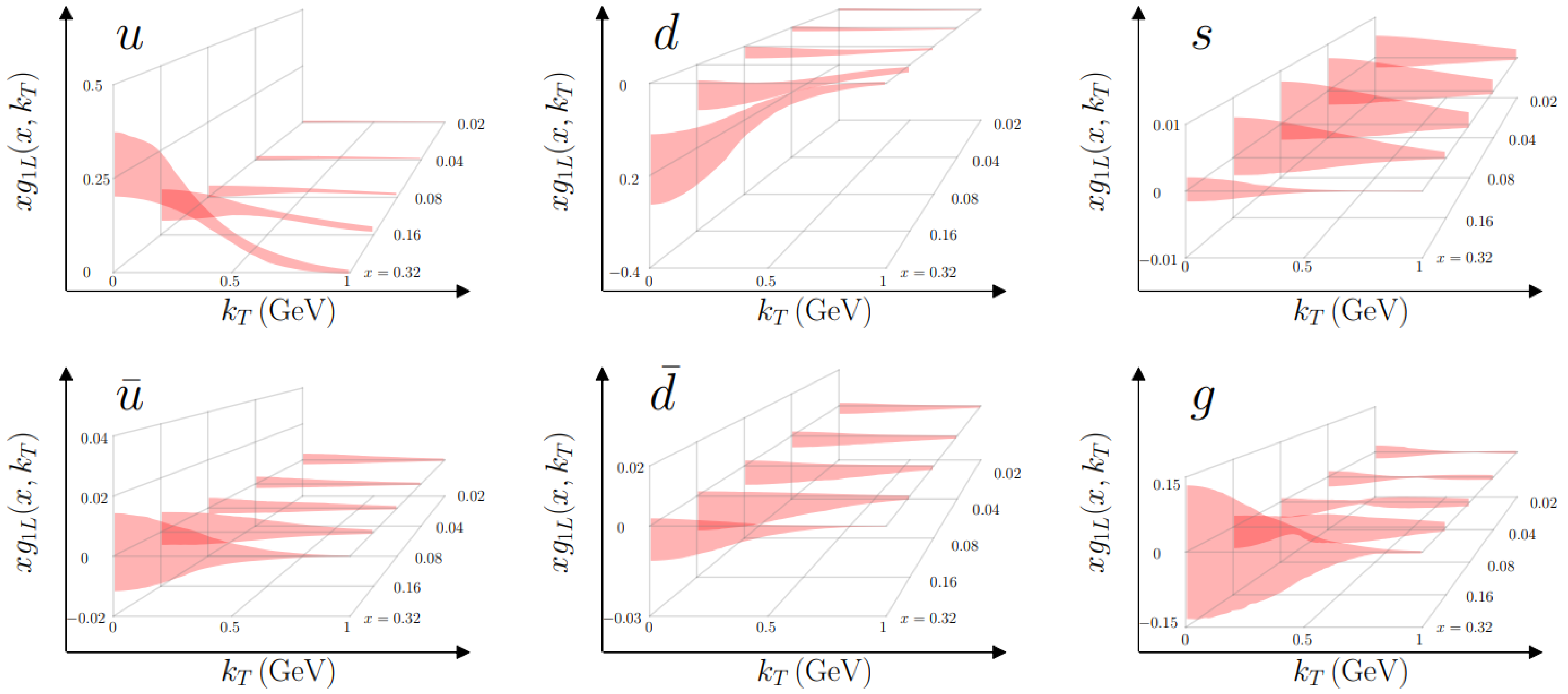

Results

Polarization of up quark and down quark:

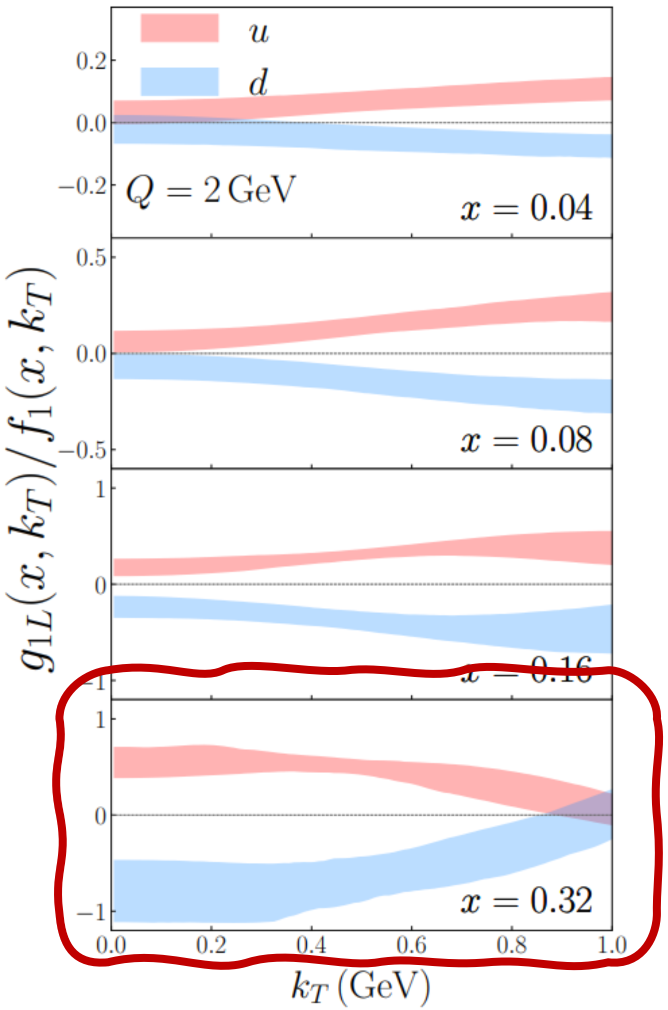

$$g_{1L}\left(x, k_T^2\right) = q_\uparrow\left(x, k_T^2\right) - q_\downarrow\left(x, k_T^2\right)$$

quantifies the net density difference between quarks with spin parallel and antiparallel to the spin of a polarized proton.

$$\frac{g_{1L}\left(x, k_T^2\right)}{f_1\left(x, k_T^2\right)} = \frac{q_\uparrow\left(x, k_T^2\right) - q_\downarrow\left(x, k_T^2\right)}{q_\uparrow\left(x, k_T^2\right) + q_\downarrow\left(x, k_T^2\right)}$$

quantifies the polarization rate of quarks.

- In the relative large region, where valence quark dominate, the polarizations decrease with increasing transverse momentum, consistent with the prediction of Melosh-Wigner rotation effect.

Results

Polarization of up quark and down quark:

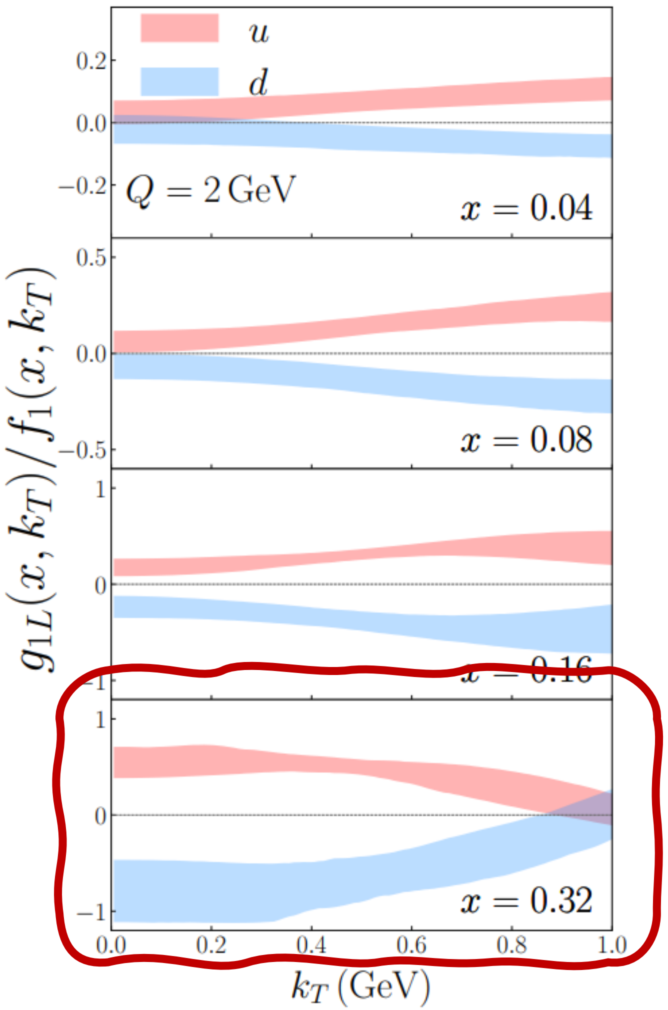

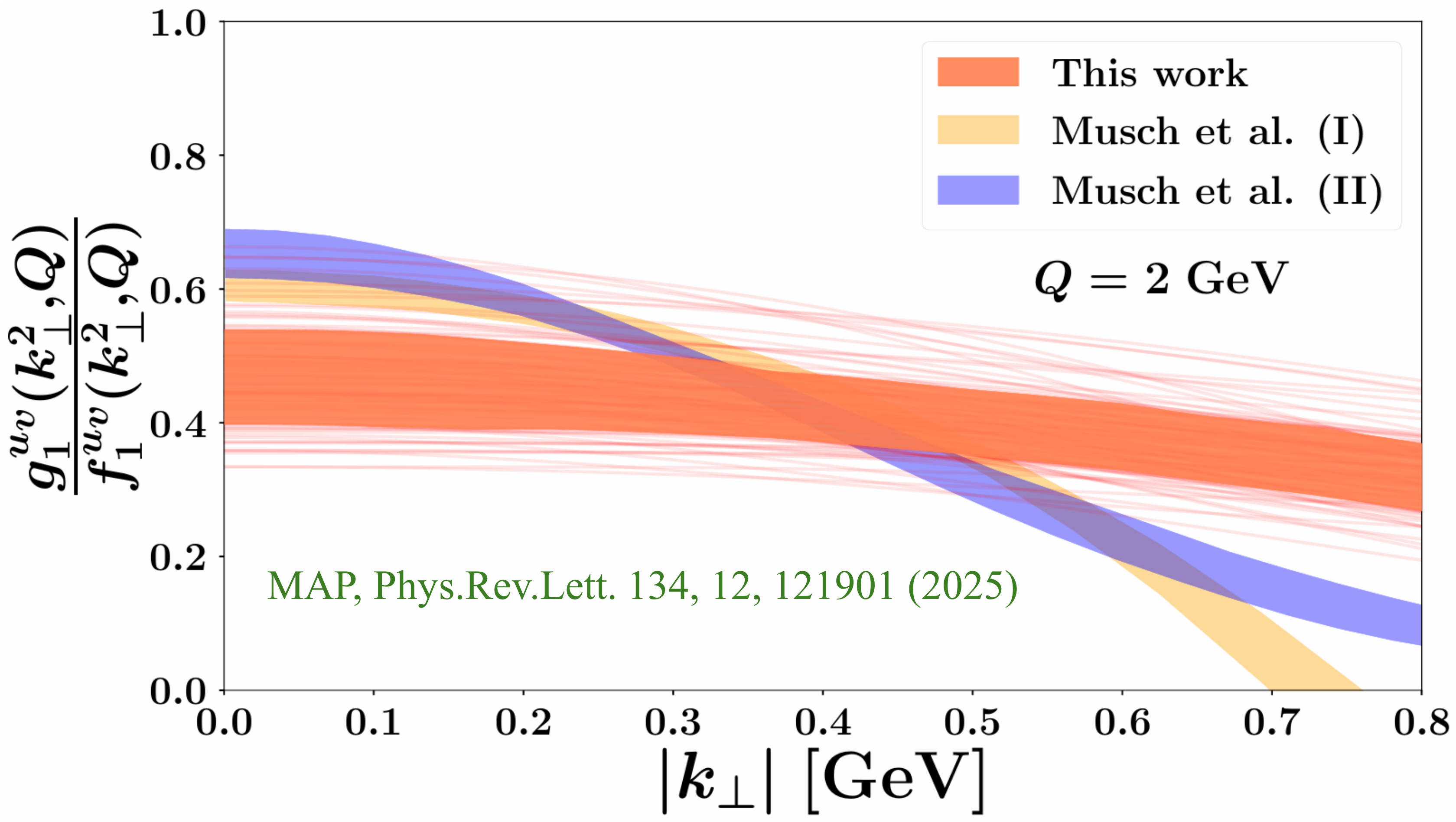

Results

Polarization of up quark and down quark:

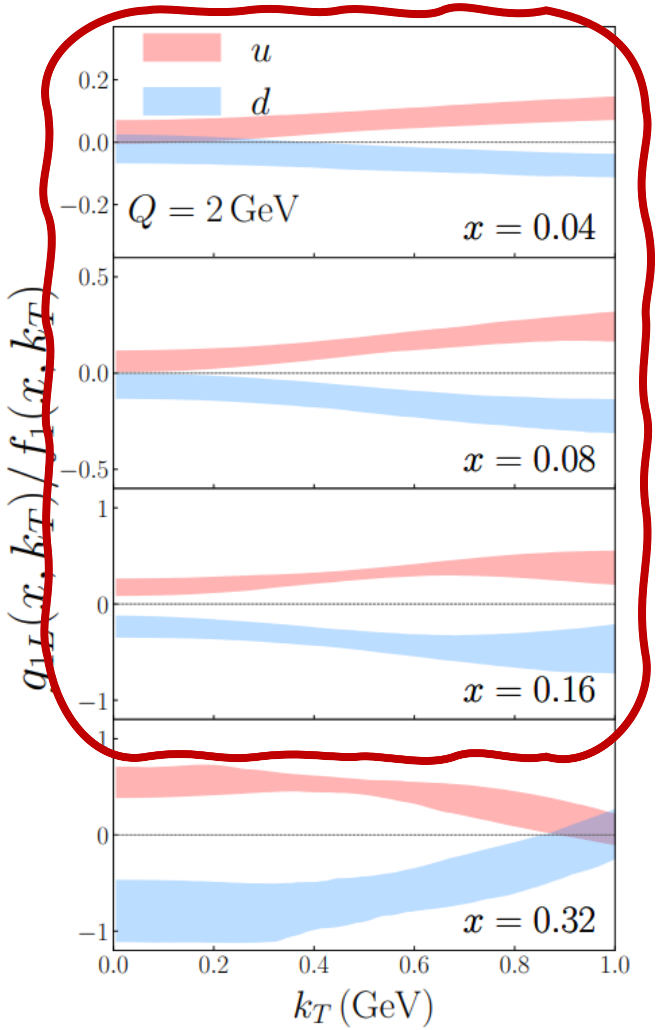

$$g_{1L}\left(x, k_T^2\right) = q_{\uparrow}\left(x, k_T^2\right) - q_{\downarrow}\left(x, k_T^2\right)$$

quantifies the net density difference between quarks with spin parallel and antiparallel to the spin of a polarized proton.

$$\frac{g_{1L}\left(x, k_T^2\right)}{f_1\left(x, k_T^2\right)} = \frac{q_{\uparrow}\left(x, k_T^2\right) - q_{\downarrow}\left(x, k_T^2\right)}{q_{\uparrow}\left(x, k_T^2\right) + q_{\downarrow}\left(x, k_T^2\right)}$$

quantifies the polarization rate of quarks.

- At lower x region, where sea quarks and gluon dominate, we observe slightly increasing polarization, which imply the rich dynamics of QCD.

Exploration of Azimuthal Modulation

$$F_{LL}^{\cos\phi} = \frac{2M}{Q}\mathcal{C}\left[\frac{\hat{\boldsymbol{h}}\cdot\boldsymbol{p}_T}{M_h}\left(xe_L H_1^\perp - \frac{M_h}{M} g_{1L}\frac{\tilde{D}^\perp}{z}\right) - \frac{\hat{\boldsymbol{h}}\cdot\boldsymbol{k}_T}{M}\left(x g_L^\perp D_1 + \frac{M_h}{M} h_{1L}^\perp \frac{\tilde{E}}{z}\right)\right] \approx -\frac{2M}{Q}\mathcal{C}\left[\frac{\hat{\boldsymbol{h}}\cdot\boldsymbol{k}_T}{M}(g_{1L}D_1)\right]$$

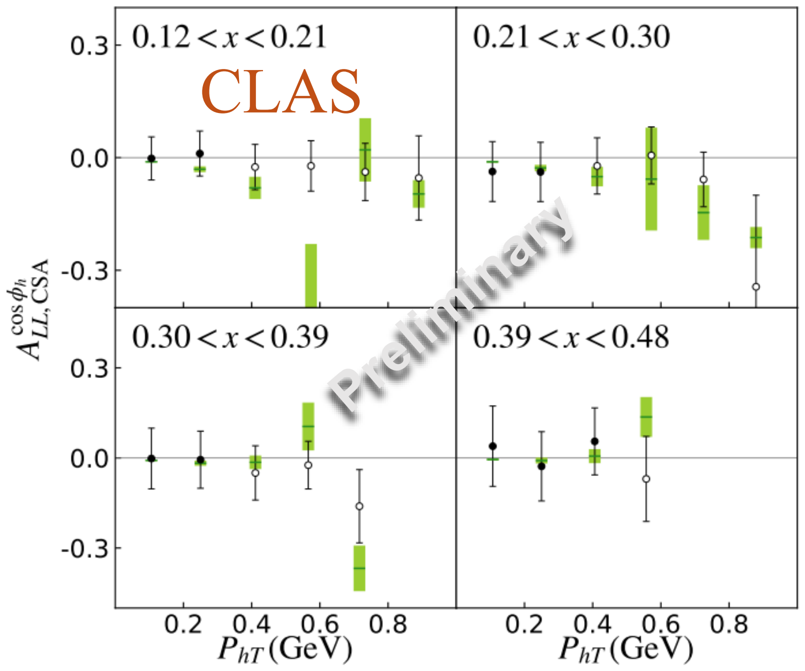

$$A_{LL}^{\cos\phi_h} = \sqrt{2\varepsilon(1-\varepsilon)}\,\frac{F_{LL}^{\cos\phi_h}}{F_{UU,T}}$$

Data set	Target	Beam	Data points	Process	χ^2/N
HERMES	H_2	27.6 GeV $e^\pm$	30(10)	$e^\pm p \to e^\pm \pi^+ X$	0.62
HERMES	H_2	27.6 GeV $e^\pm$	30(11)	$e^\pm p \to e^\pm \pi^- X$	0.74
HERMES	D_2	27.6 GeV $e^\pm$	30(10)	$e^\pm d \to e^\pm \pi^+ X$	0.81
HERMES	D_2	27.6 GeV $e^\pm$	30(9)	$e^\pm d \to e^\pm \pi^- X$	1.03
HERMES	D_2	27.6 GeV $e^\pm$	30(10)	$e^\pm d \to e^\pm K^+ X$	0.96
HERMES	D_2	27.6 GeV $e^\pm$	30(10)	$e^\pm d \to e^\pm K^- X$	0.58
CLAS	$^{14}NH_3$	6 GeV e^-	21(9)	$e^- p \to e^- \pi^0 X$	0.11
Total			201(69)		0.70

Preliminary

The TMD helicity extracted can also explain the $\cos\phi_h$ modulation of the DSA measurement of the SIDIS.

Polarized Electron Ion Collider in China (EicC)

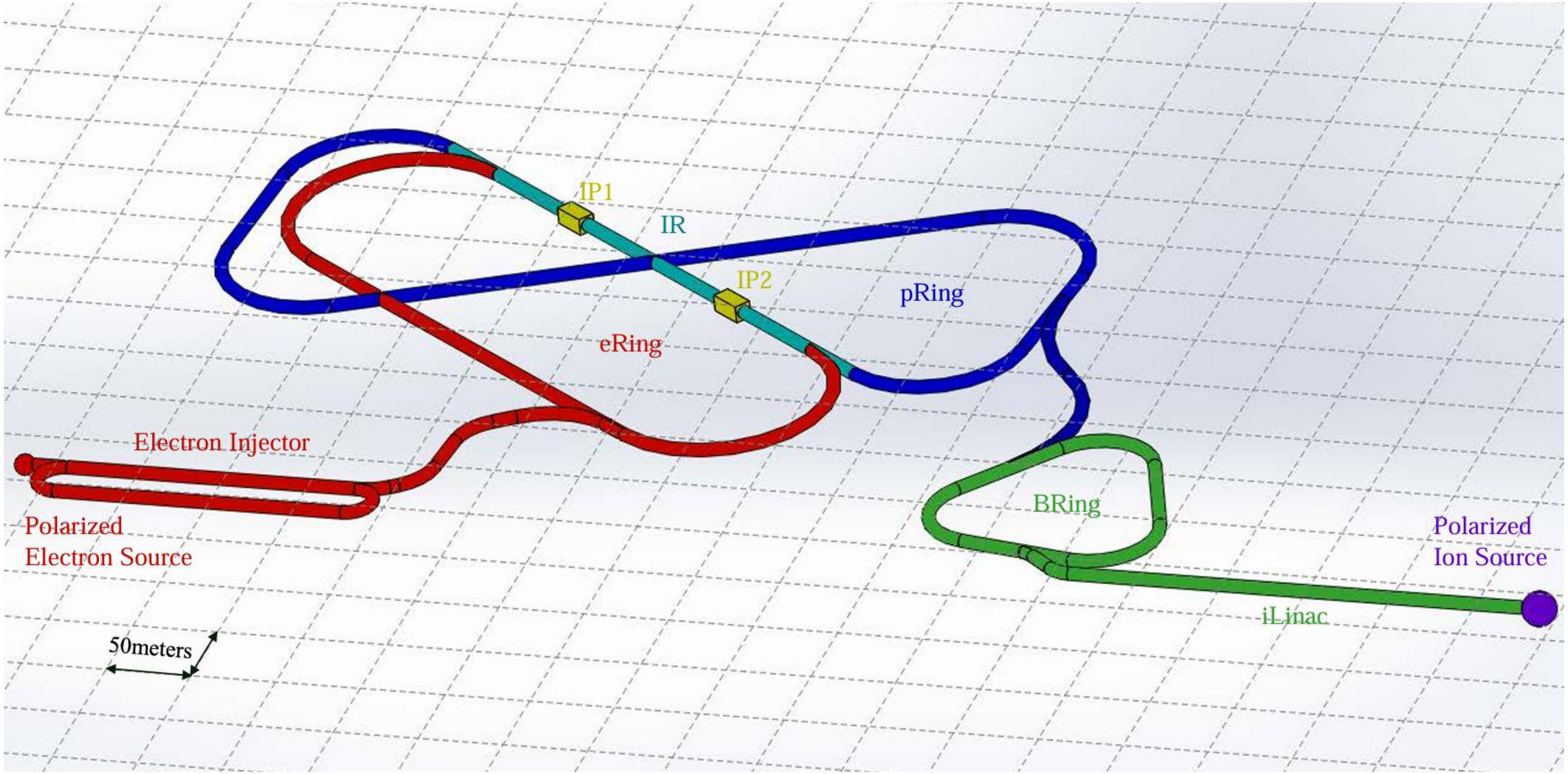

D. P. Anderle *et al.* Front.Phys.(Beijing) 16 (2021) 6, 64701

Polarized Electron Ion Collider in China (EicC)

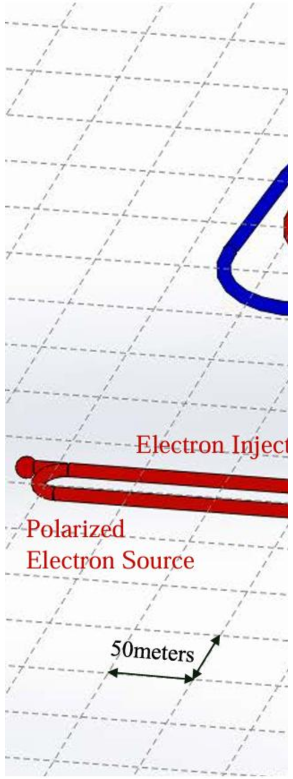

Table 1.1: Available particles and their corresponding energy, polarization, luminosity and integrated luminosity.

Particle	Momentum (GeV/c/u)	CM energy (GeV/u)	Average Polarization	Luminosity at the nucleon level ($cm^{-2}s^{-1}$)	Integrated luminosity (fb^{-1})
e	3.5		80%		
p	20	16.76	70%	2.00×10^{33}	50.5
d	12.90	13.48	Yes	8.48×10^{32}	21.4
$^{3}He^{++}$	17.21	15.55	Yes	6.29×10^{32}	15.9
$^{7}Li^{3+}$	11.05	12.48	No	9.75×10^{32}	24.6
$^{12}C^{6+}$	12.90	13.48	No	8.35×10^{32}	21.1
$^{40}Ca^{20+}$	12.90	13.48	No	8.35×10^{32}	21.1
$^{197}Au^{79+}$	10.35	12.09	No	9.37×10^{32}	23.6
$^{208}Pb^{82+}$	10.17	11.98	No	9.22×10^{32}	23.3
$^{238}U^{92+}$	9.98	11.87	No	8.92×10^{32}	22.5

D. P. Anderle *et al.* Front.Phys.(Beijing) 16 (2021) 6, 64701

Polarized Electron Ion Collider in China (EicC)

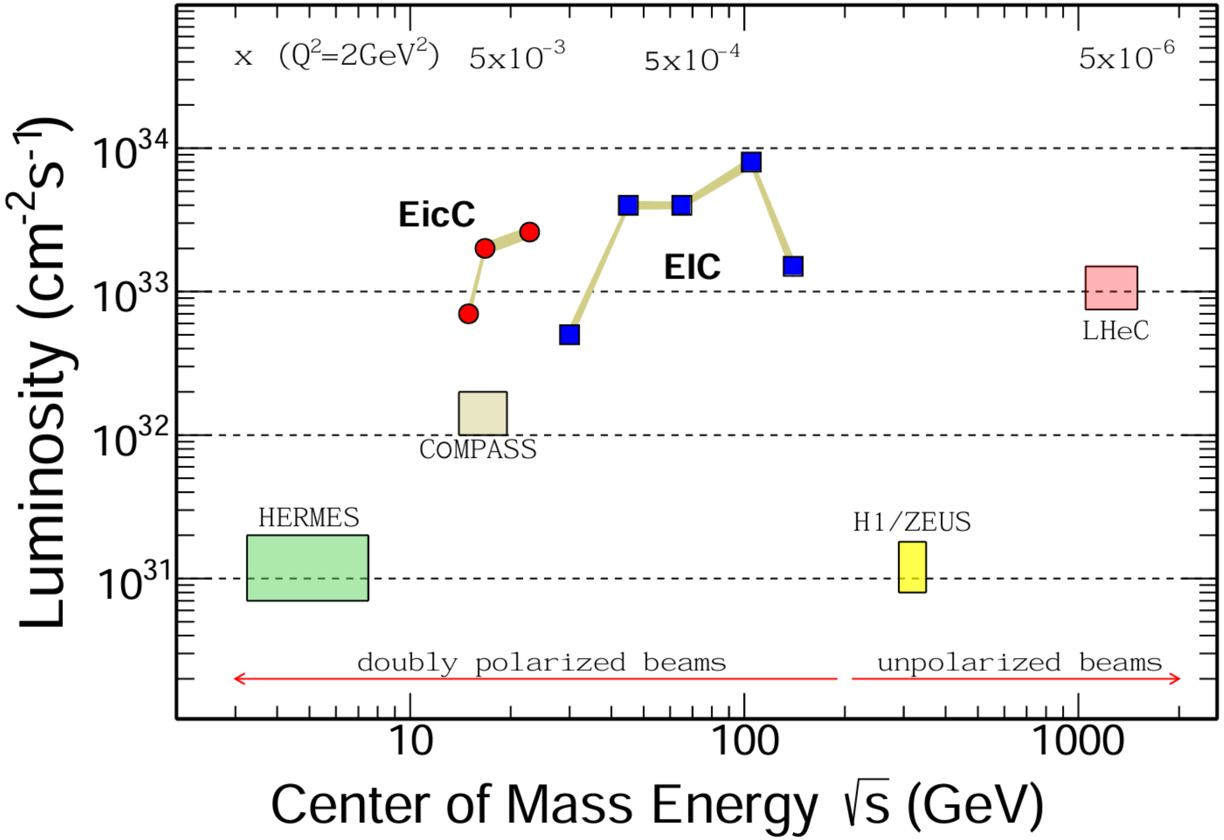

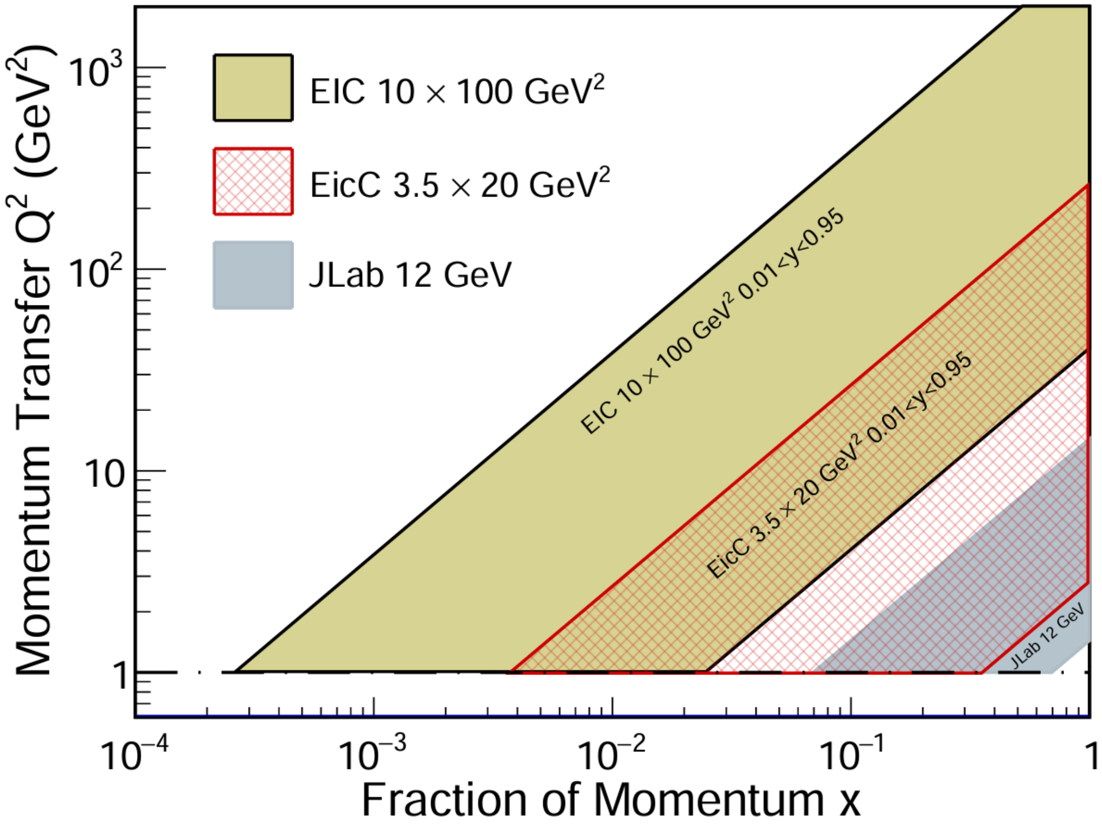

D. P. Anderle *et al.* Front.Phys.(Beijing) 16 (2021) 6, 64701

EicC Projection Results

Result of 3D helicity distributions:

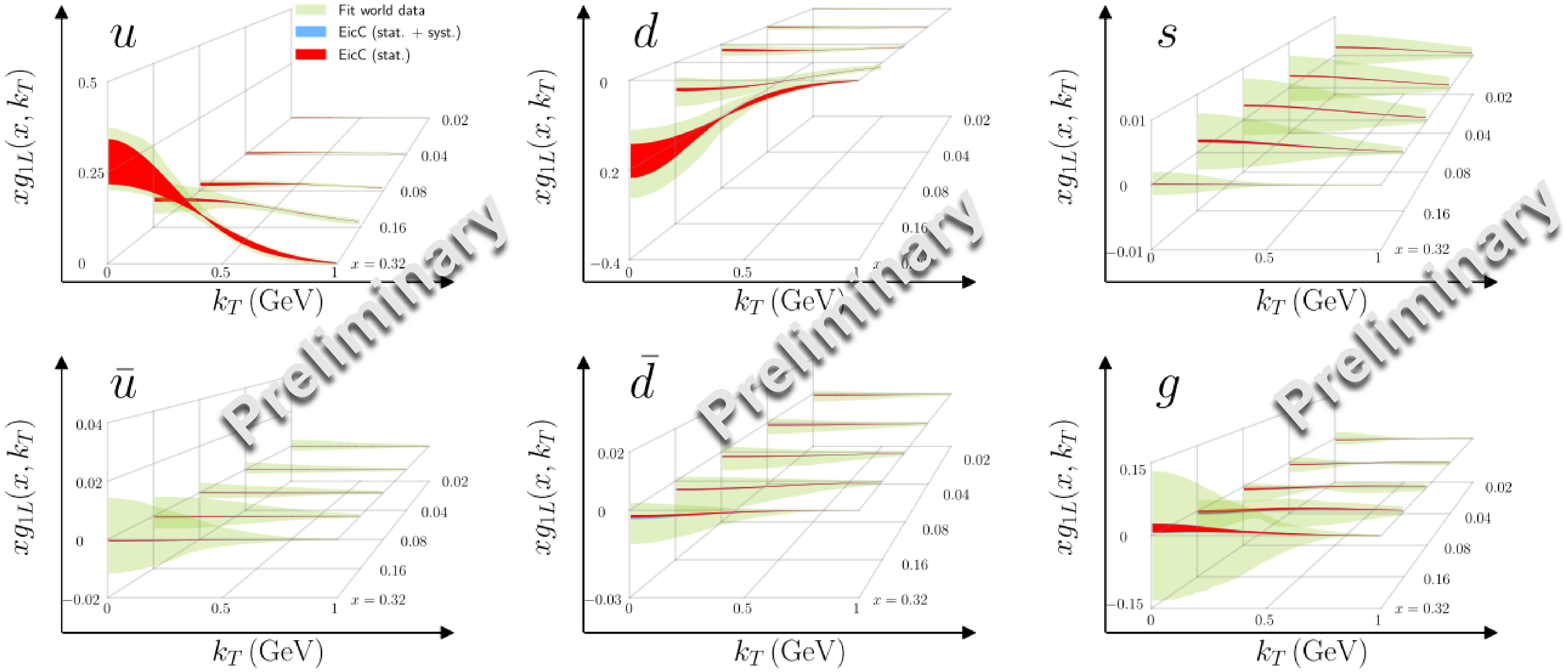

The proposed EicC will enhance the precision of sea quark and gluon helicity distributions.

EicC Projection Results

Result of zeroth moment

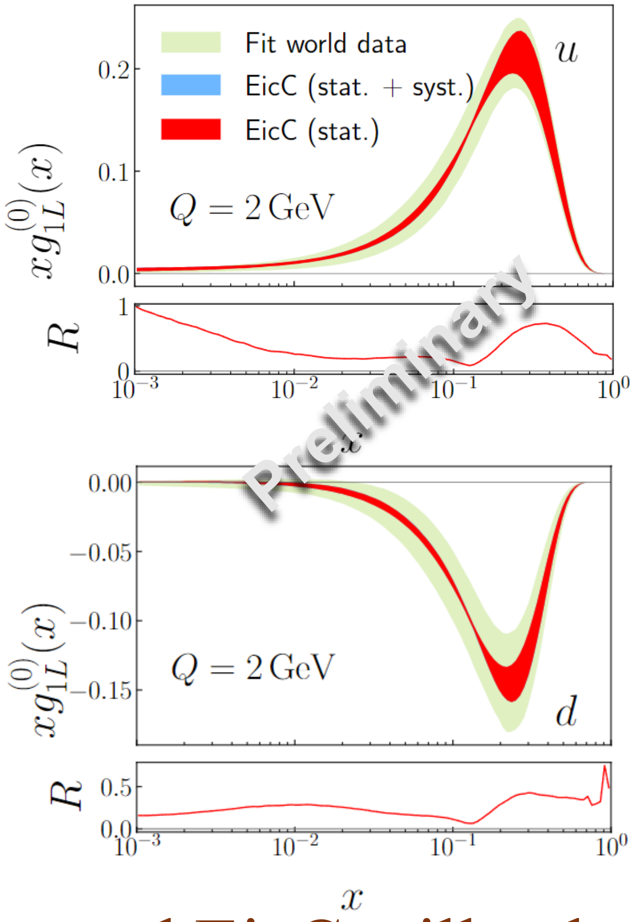

Result of parton polarization:

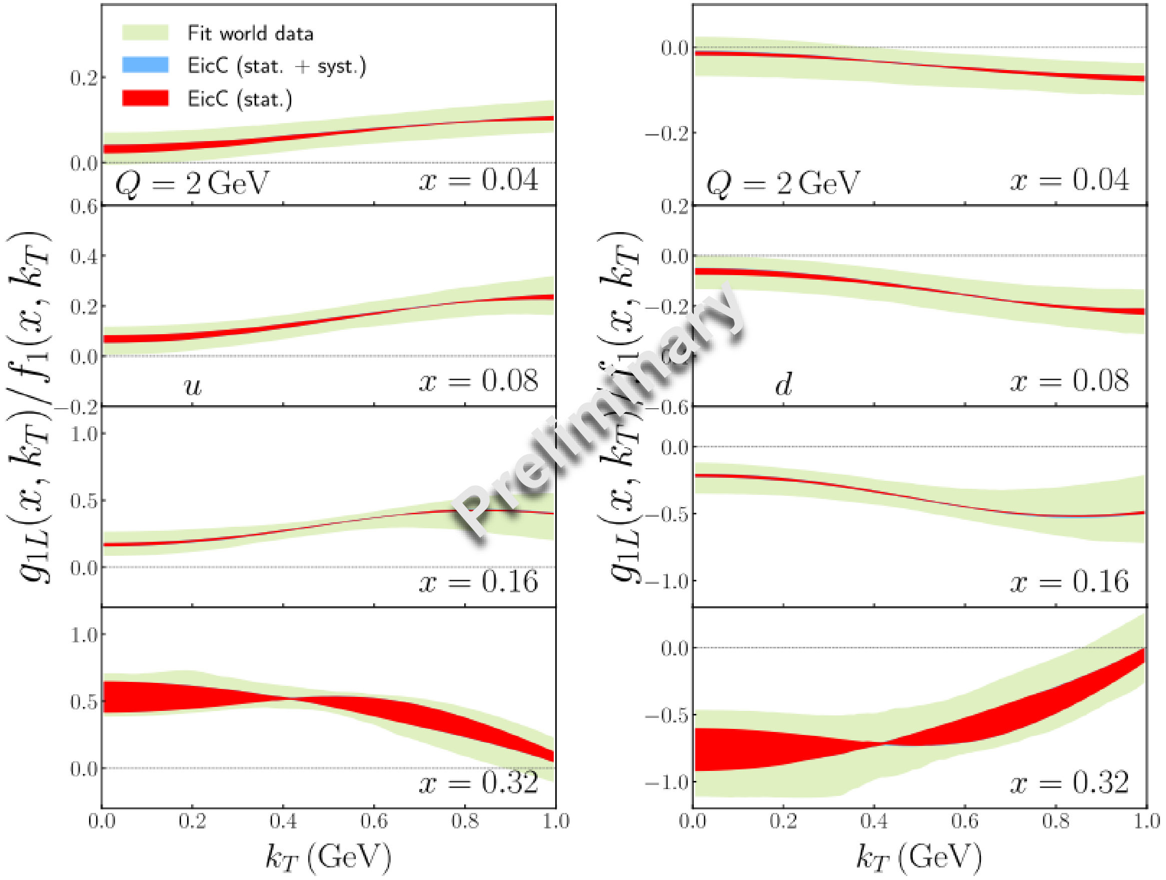

The proposed EicC will enhance the precision of helicity distribution especially among the range $x \sim 0.01 - 0.5$

Summary

- We extracted the TMD helicity functions with error bands from SIDIS data;
- Around the peak of x dependence, the polarization is concentrated on the low k_T region, which is consistent with Melosh Wigner rotation;
- At lower x region, we observe slightly increasing polarization, which imply the rich dynamics of QCD;
- Helicity distribution extracted can also explain $\cos\phi_h$ modulation data without including them;
- The proposed EicC will enhance the precision of three-dimensional helicity distribution, especially among the range x~0.01-0.5.

Thank you!

Backup——Comparison with Data

HERMES:

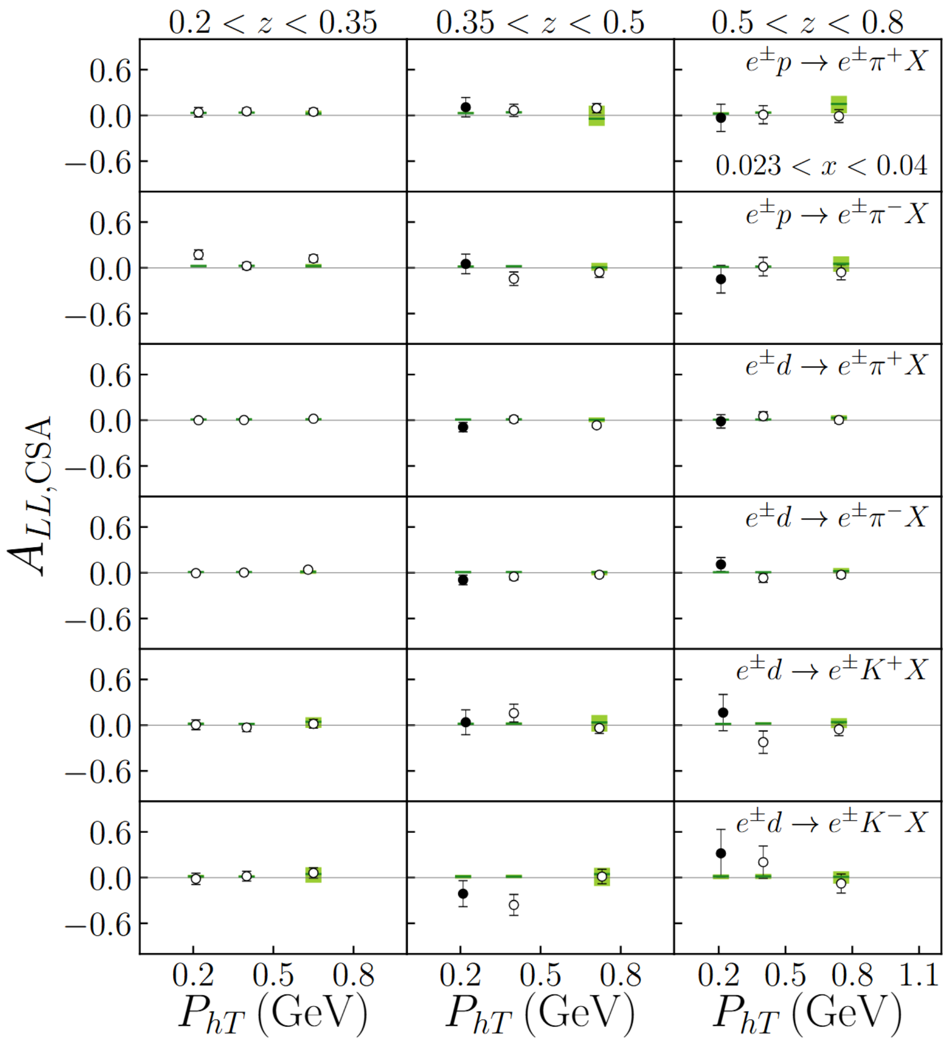

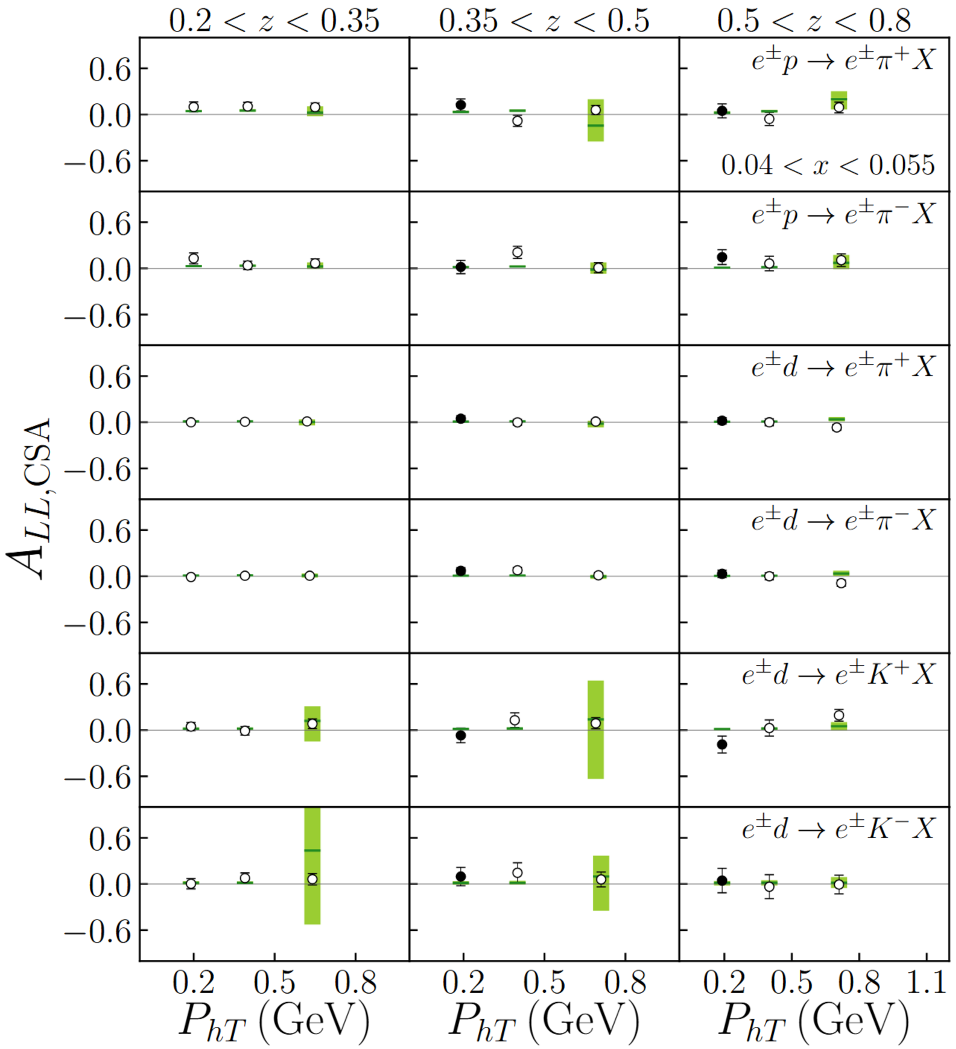

Backup——Comparison with Data

HERMES:

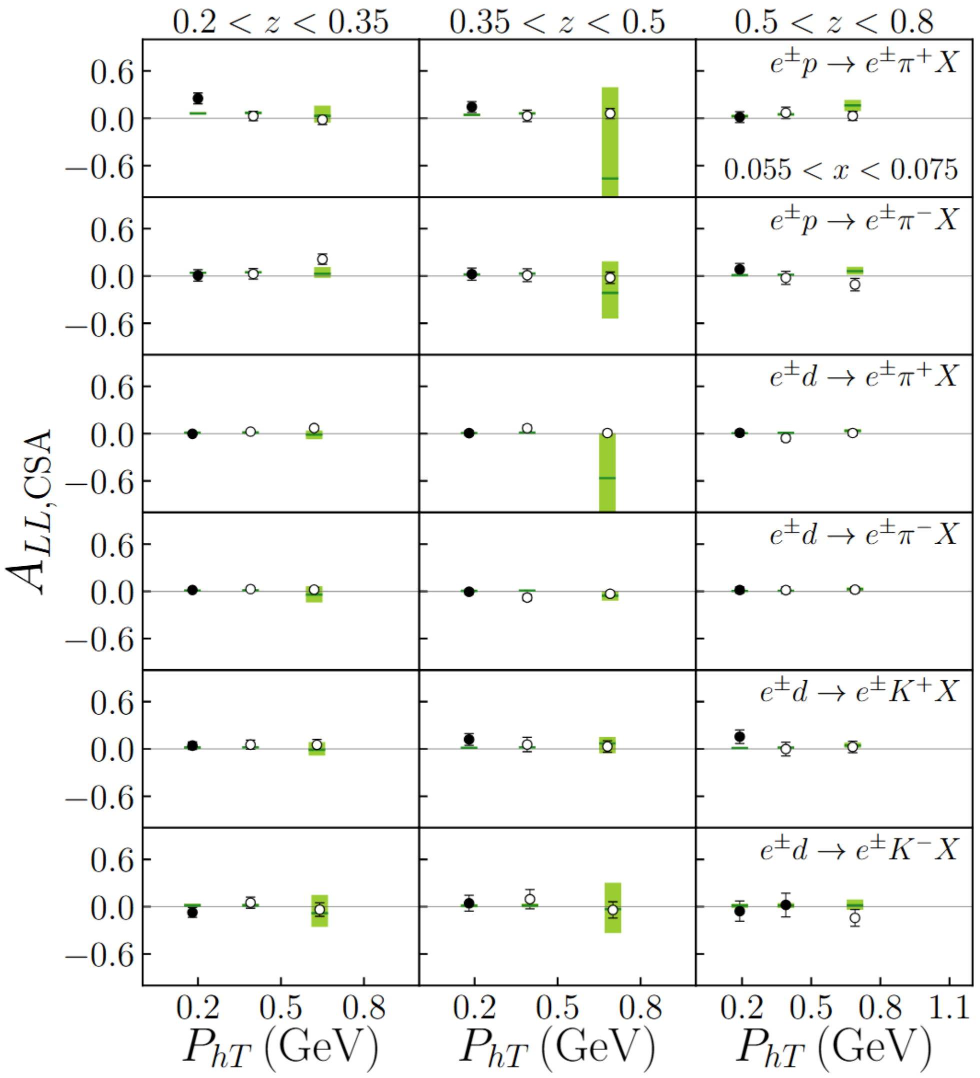

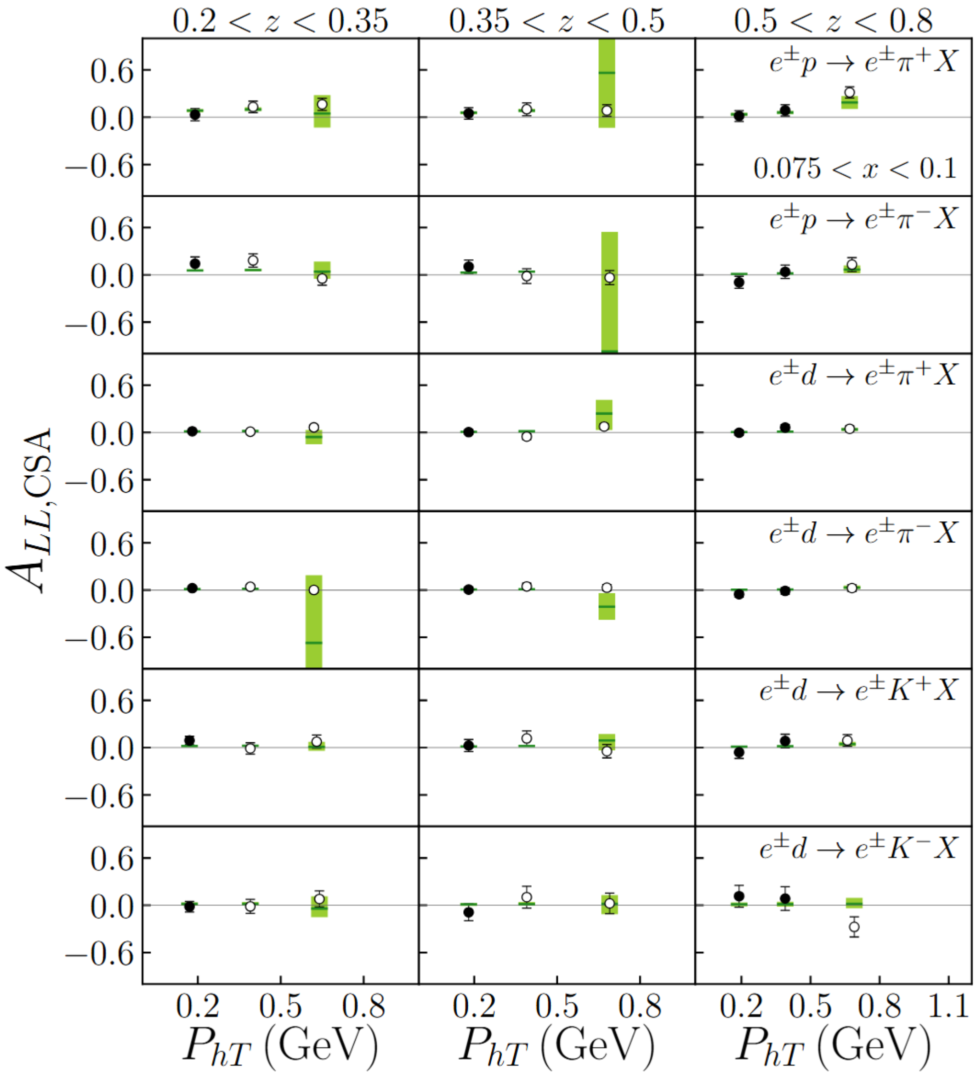

Backup——Comparison with Data

HERMES:

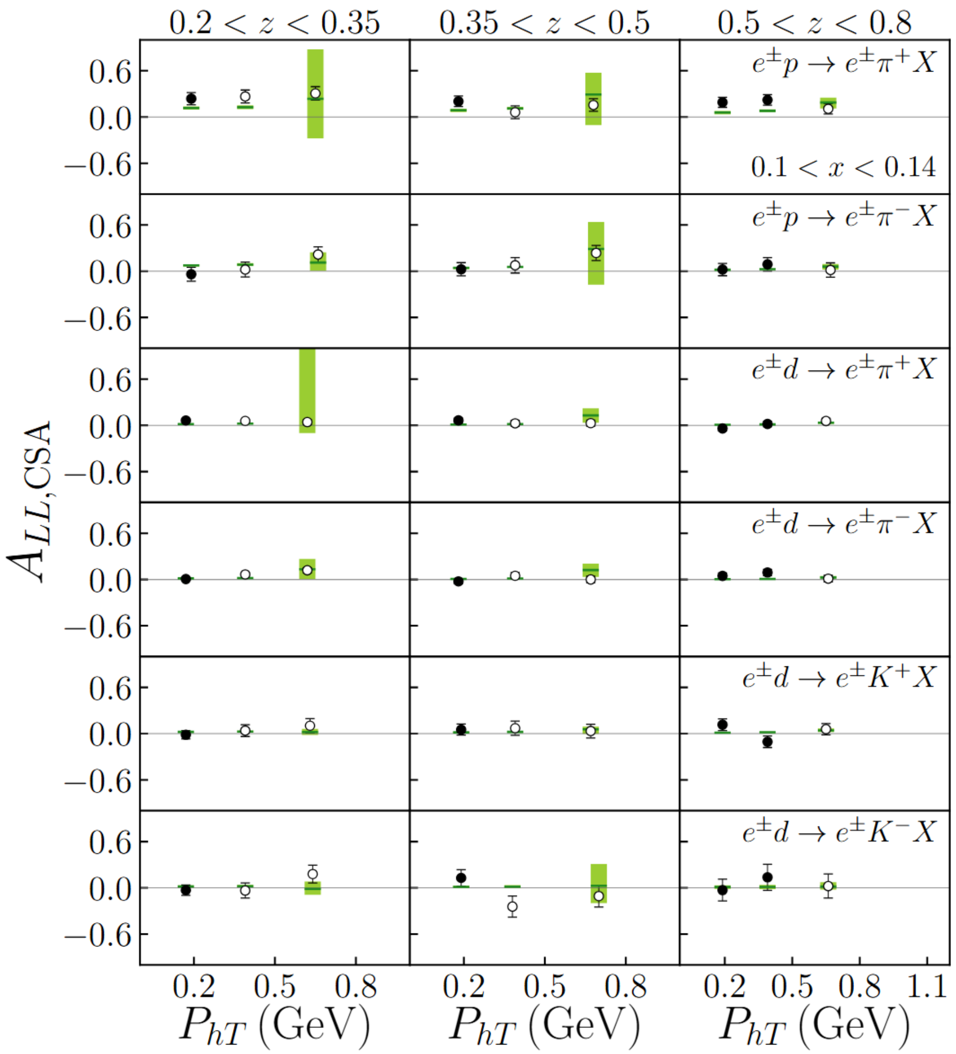

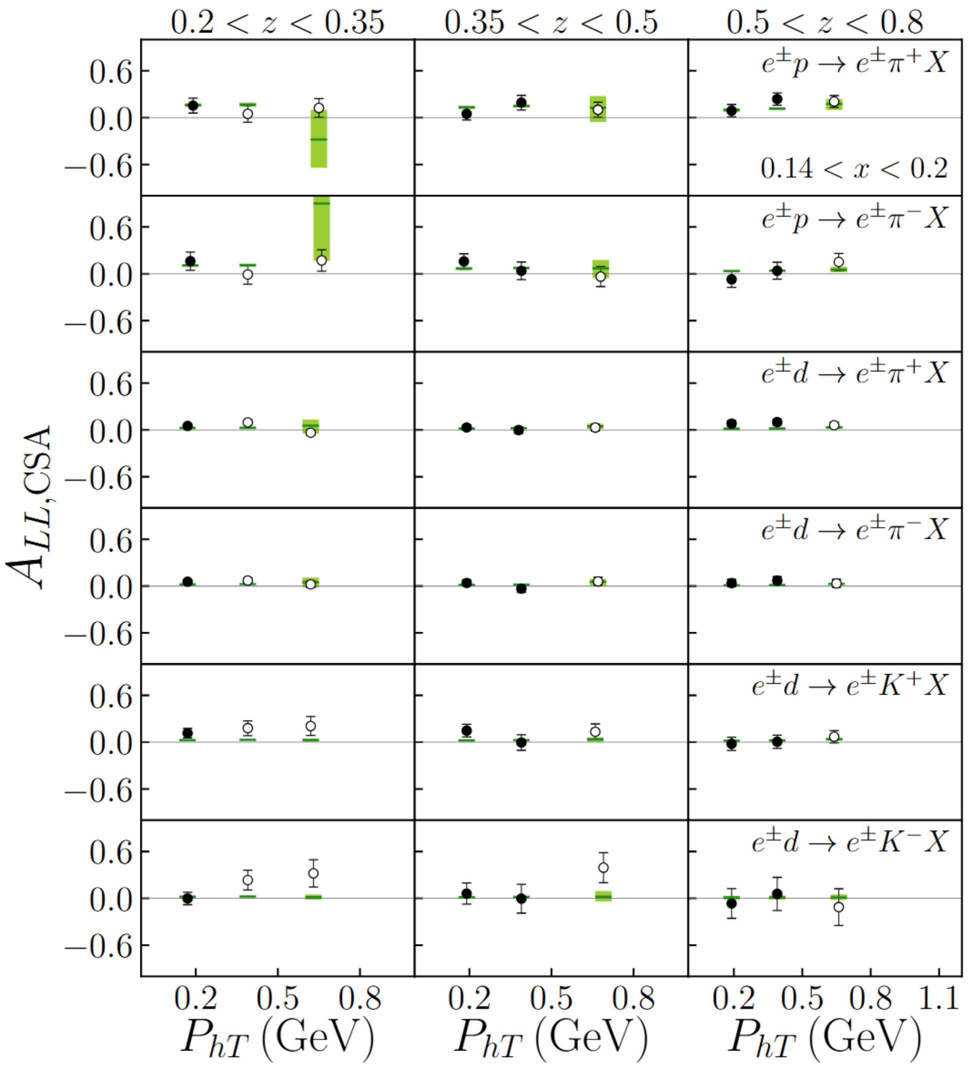

Backup——Comparison with Data

HERMES:

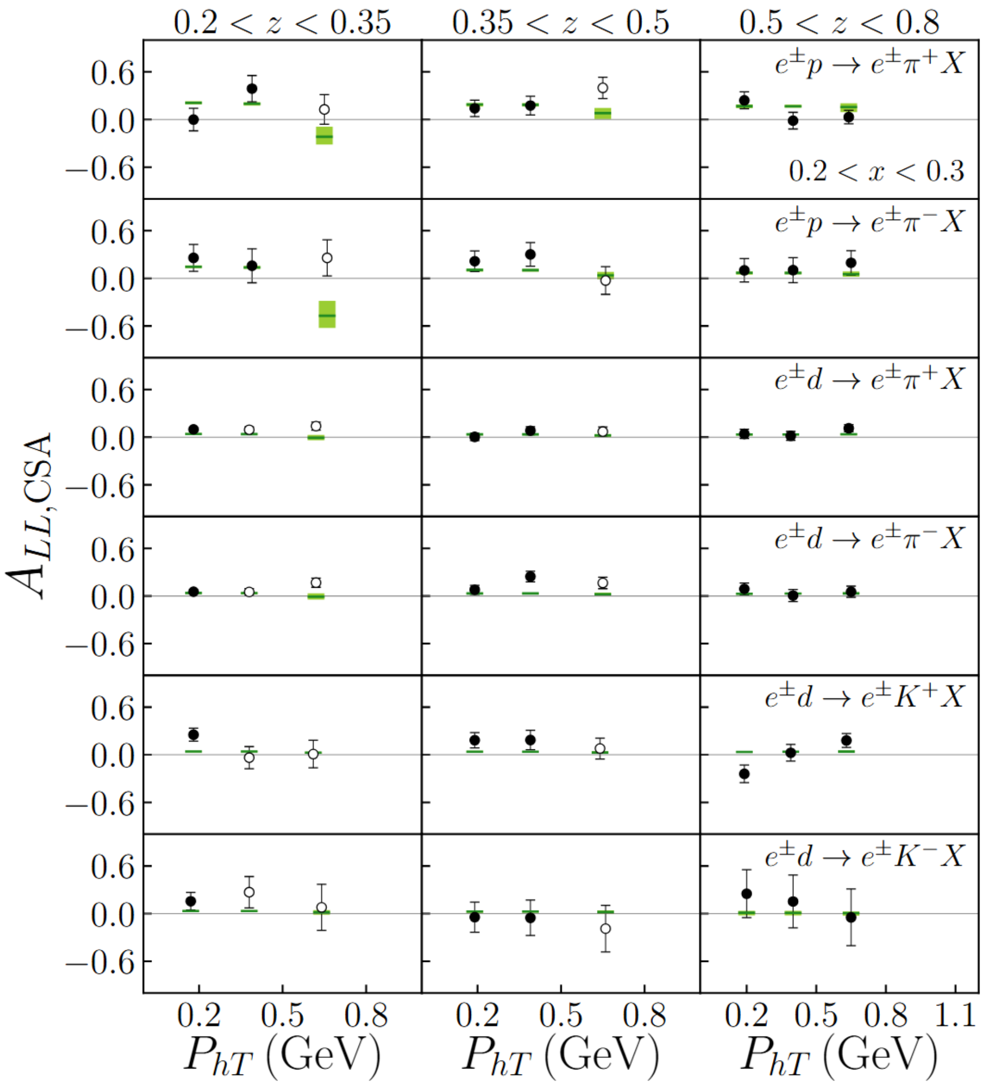

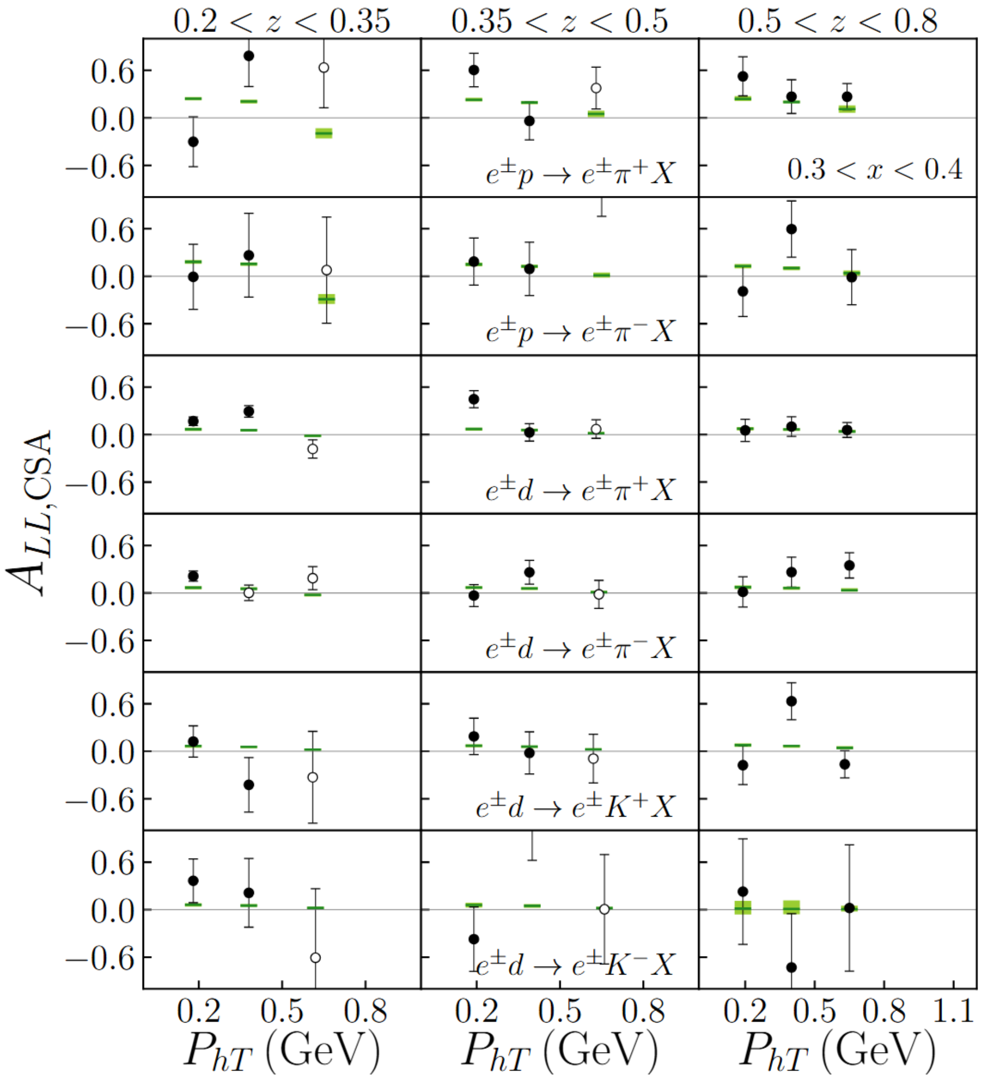

Backup——Comparison with Data

HERMES:

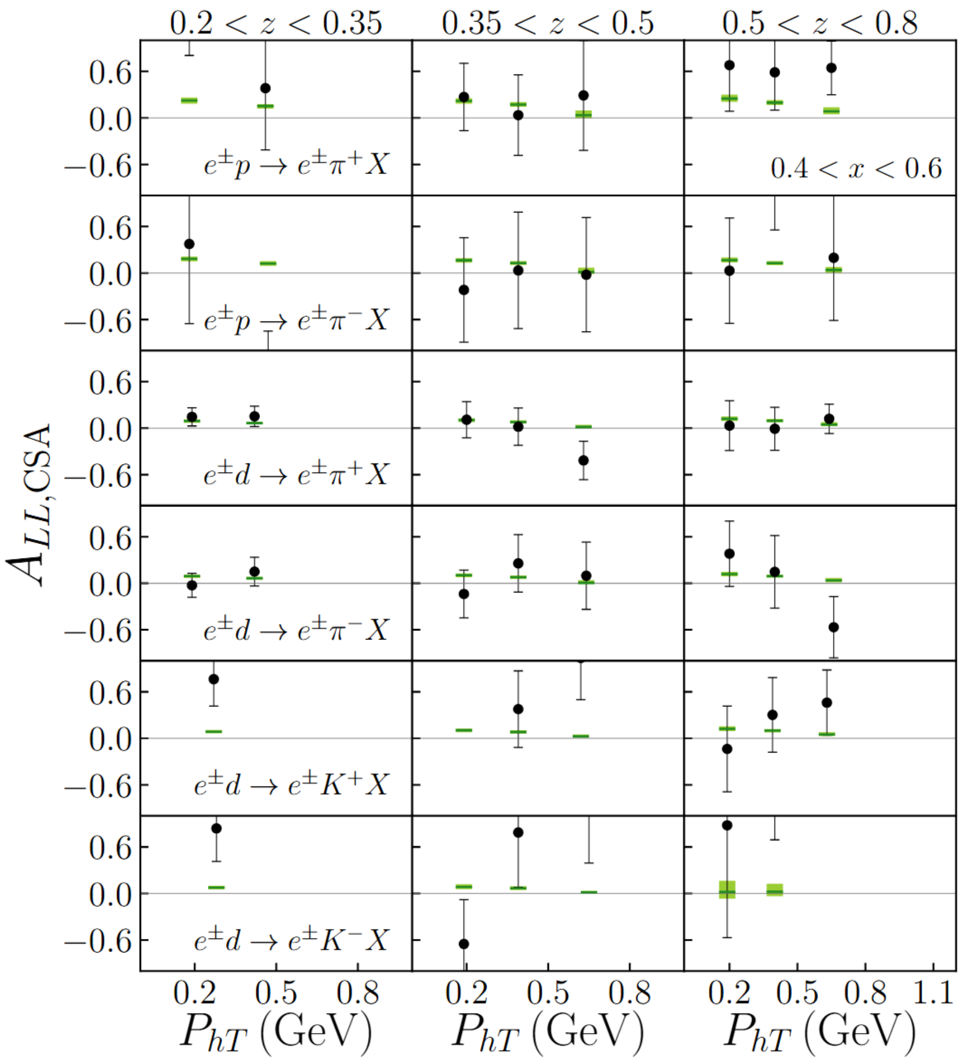

CLAS:

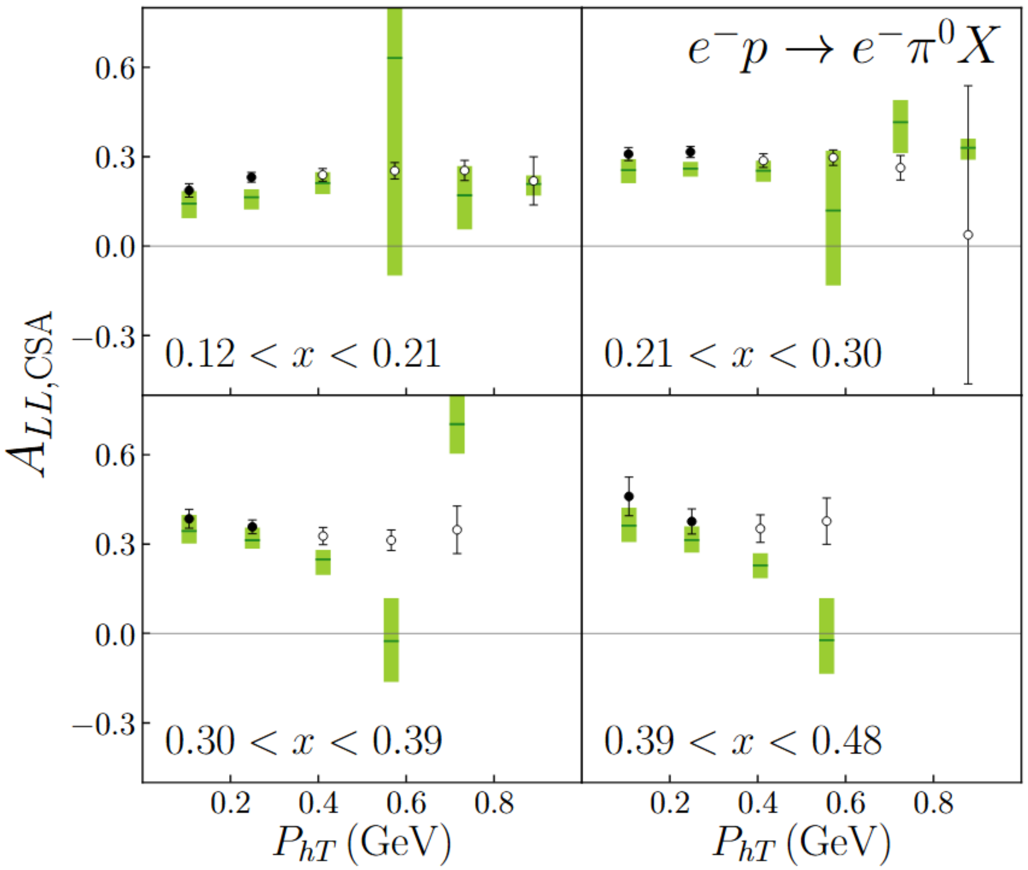

Backup——Comparison with Data: $\cos\phi_h$ Modulation

HERMES:

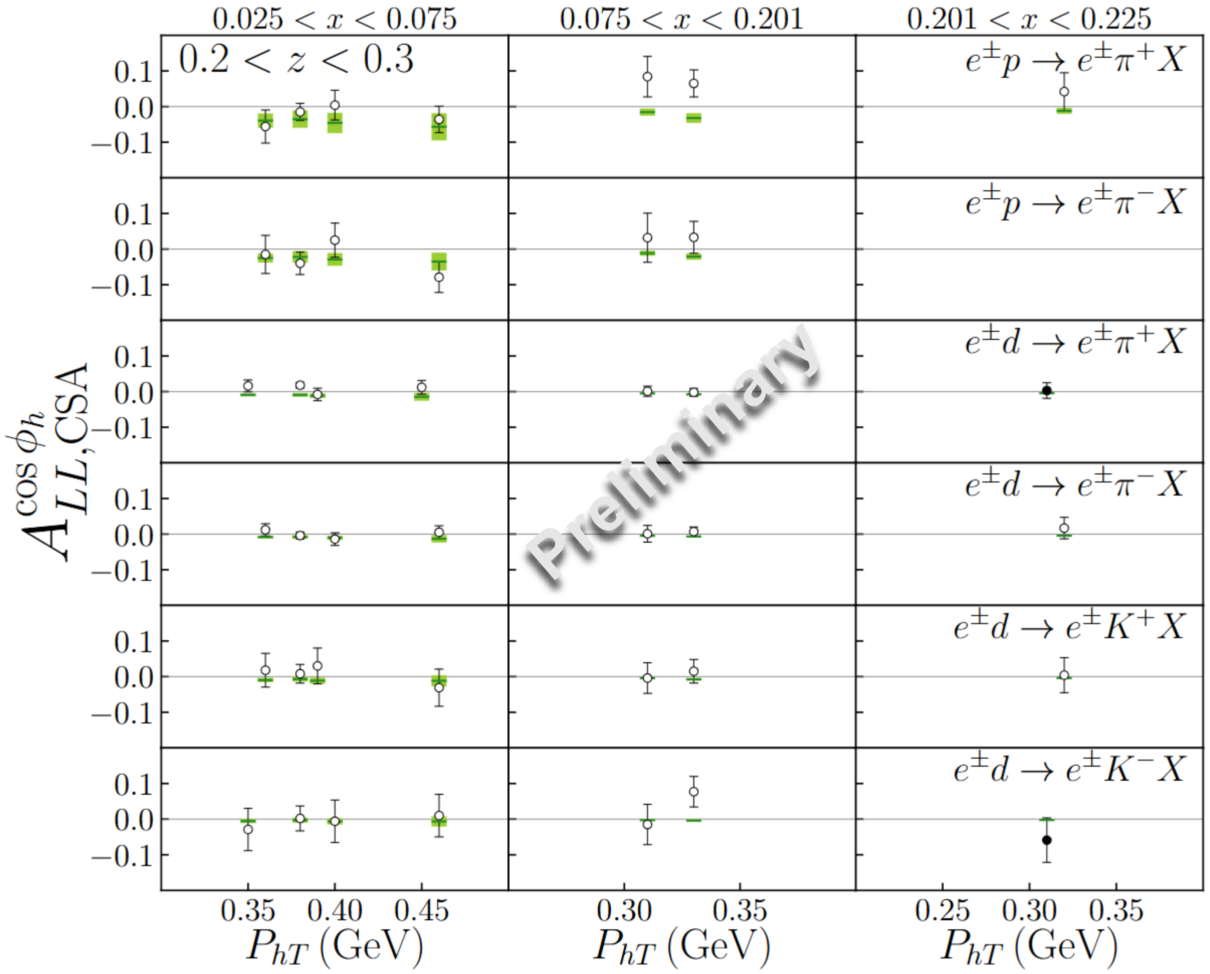

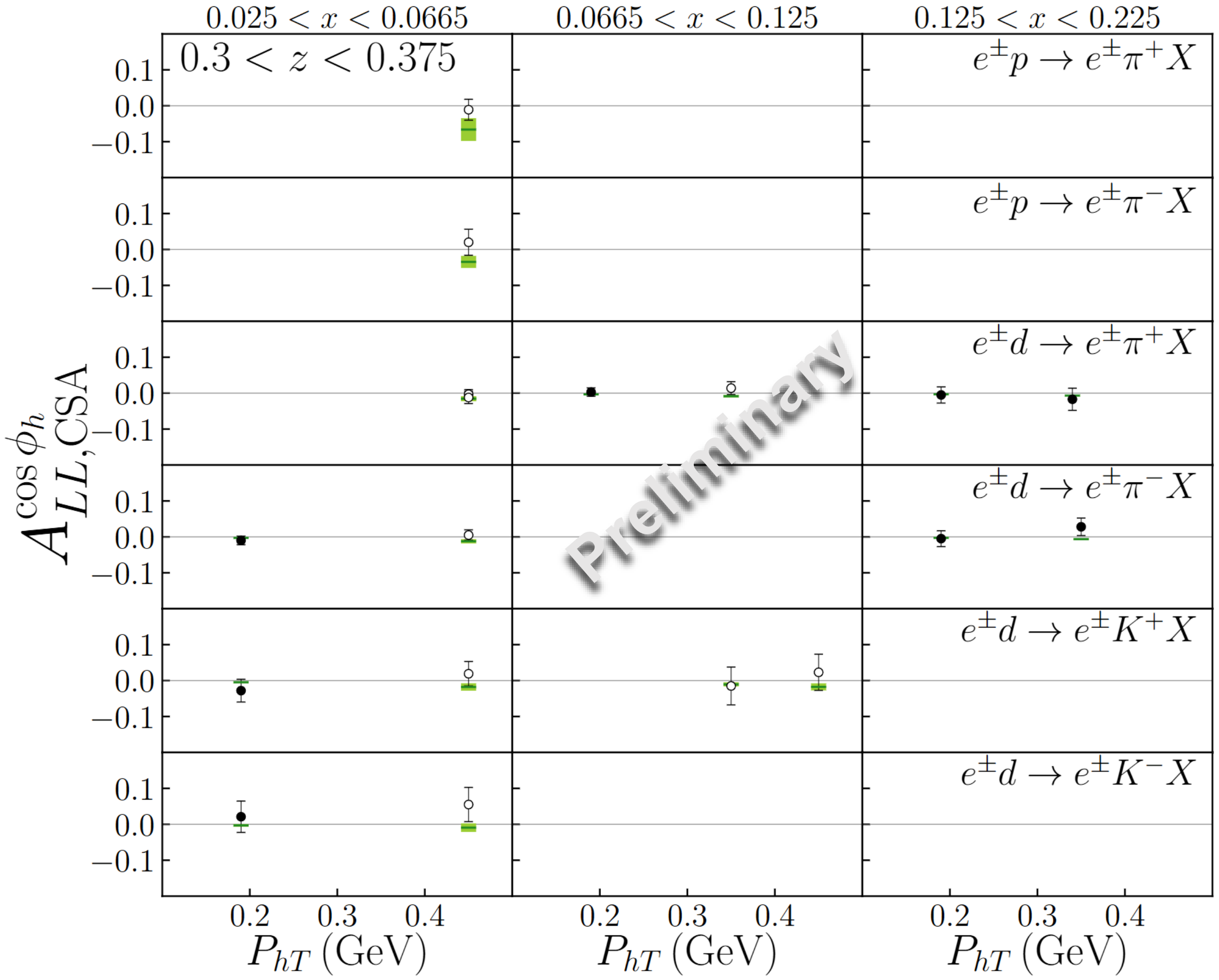

Backup——Comparison with Data: $\cos\phi_h$ Modulation

HERMES:

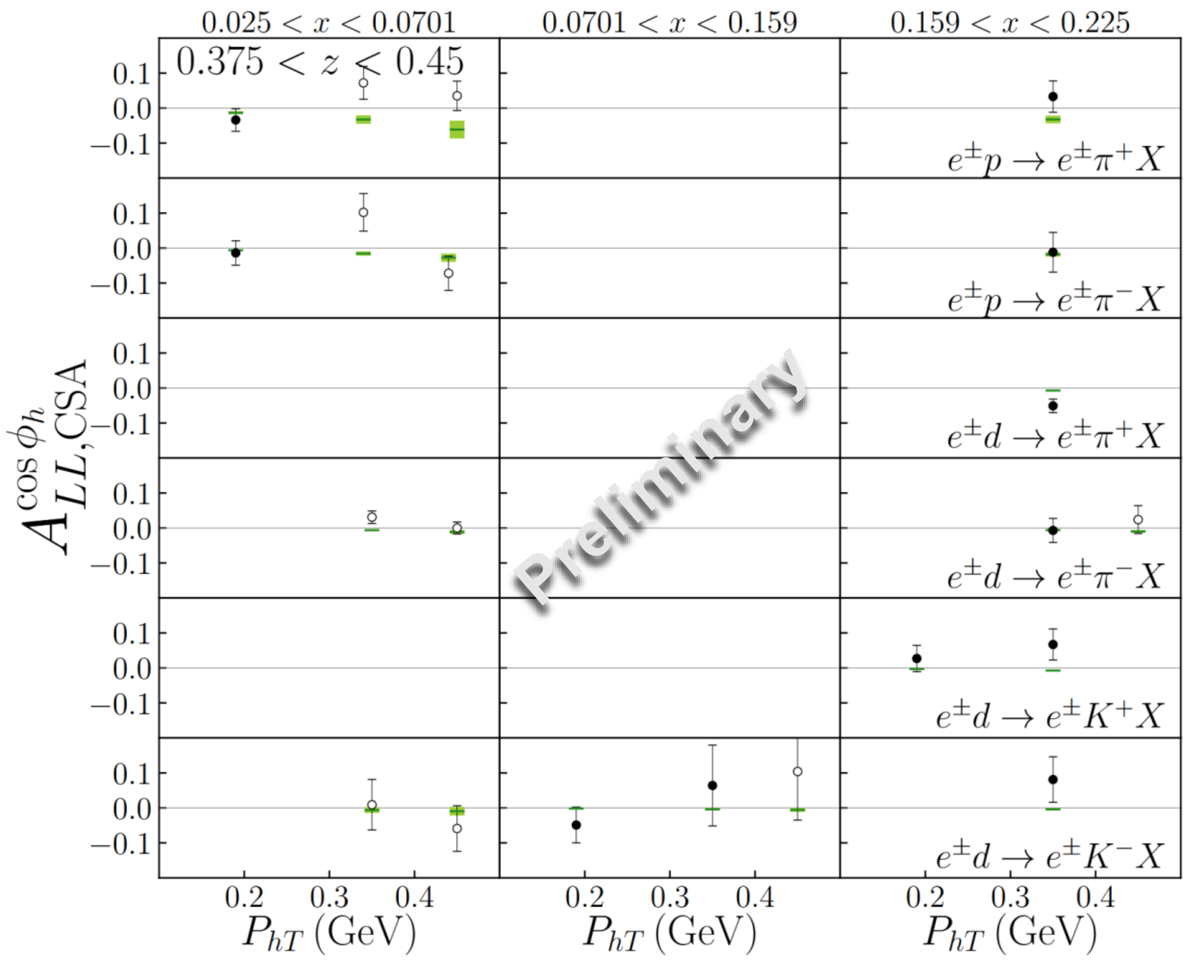

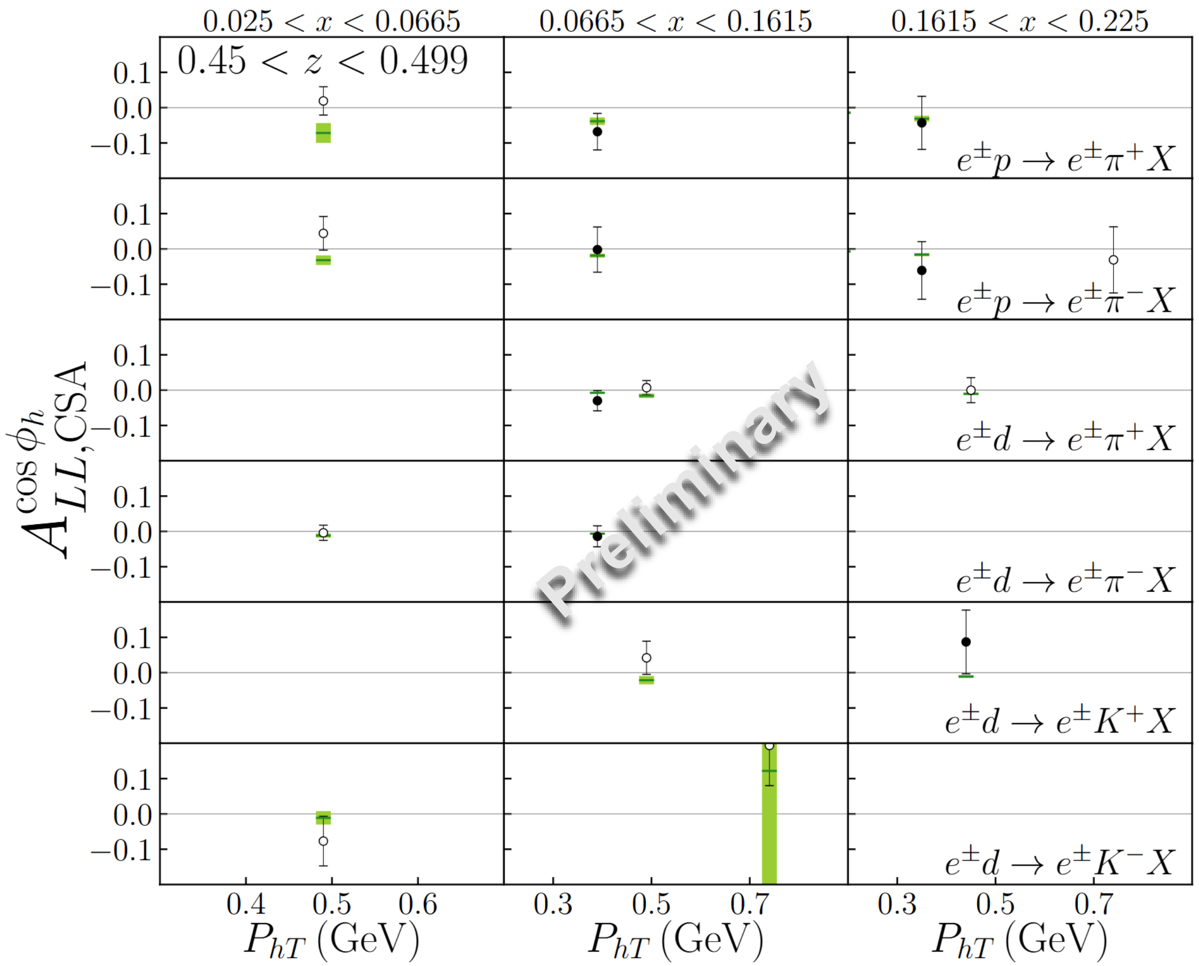

Backup——Comparison with Data: $\cos\phi_h$ Modulation

HERMES:

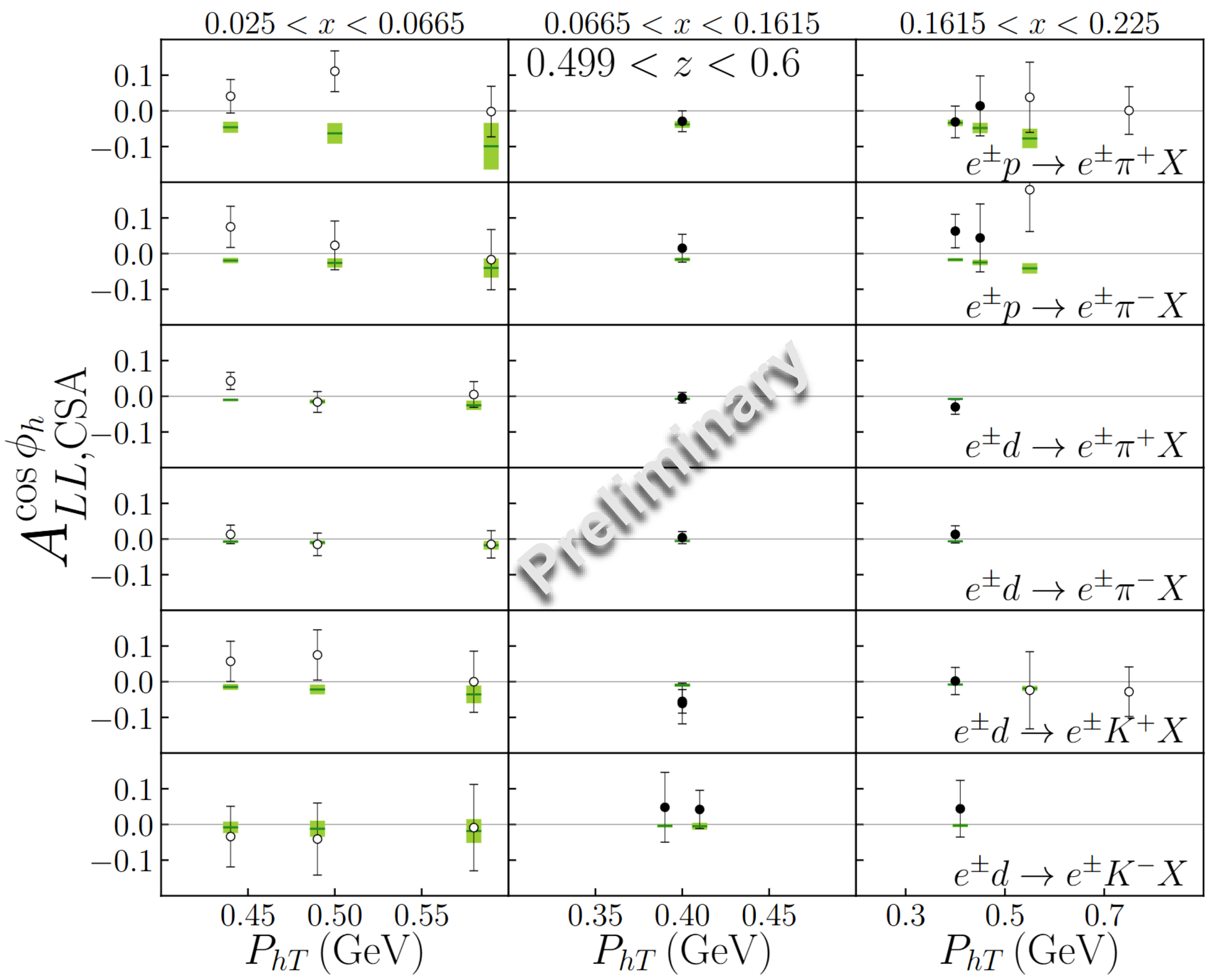

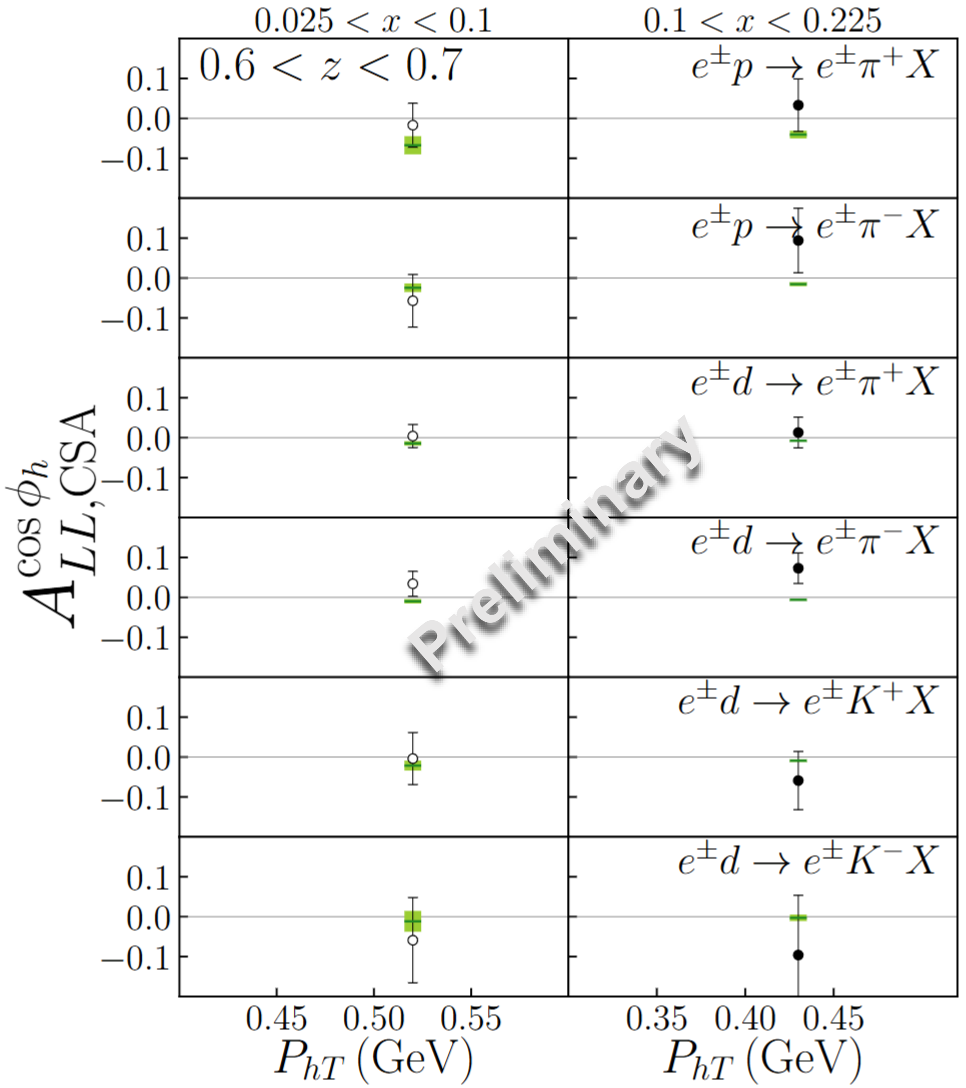

Backup——Comparison with Data: $\cos\phi_h$ Modulation

HERMES:

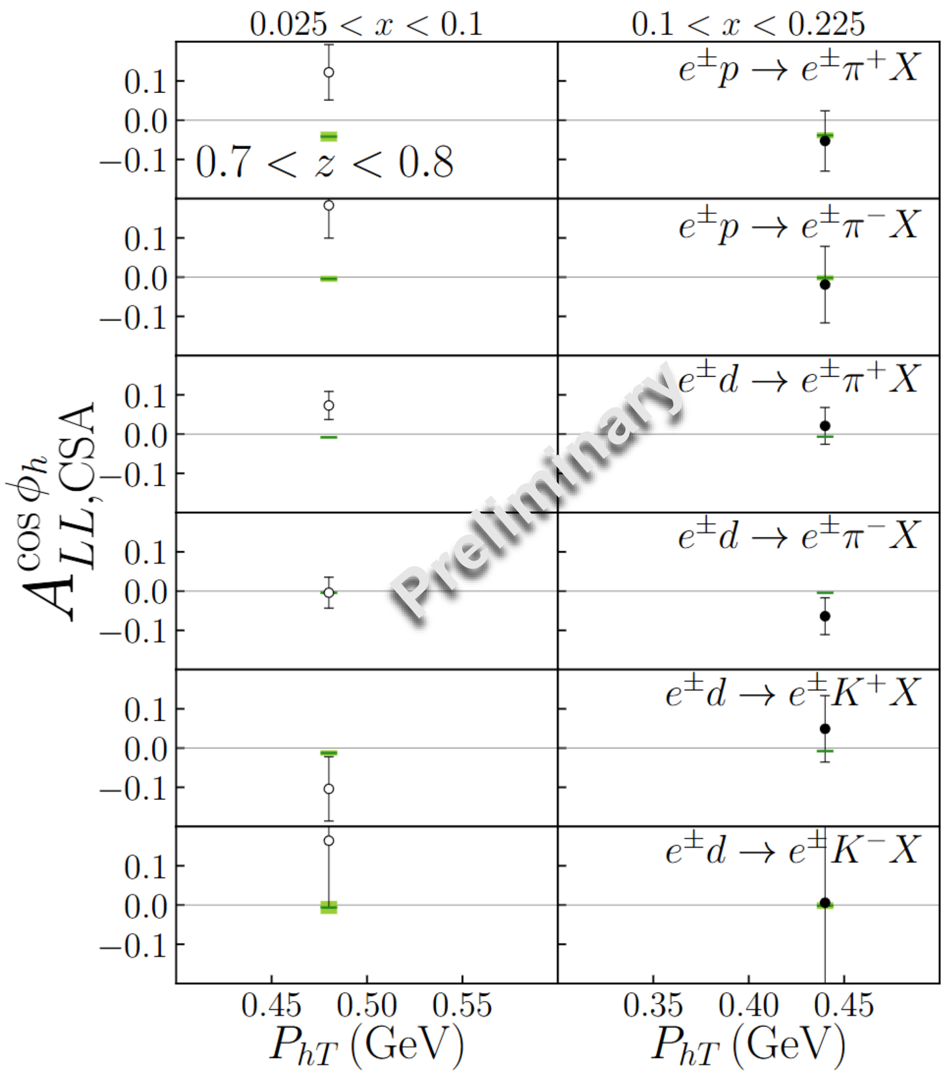

CLAS:

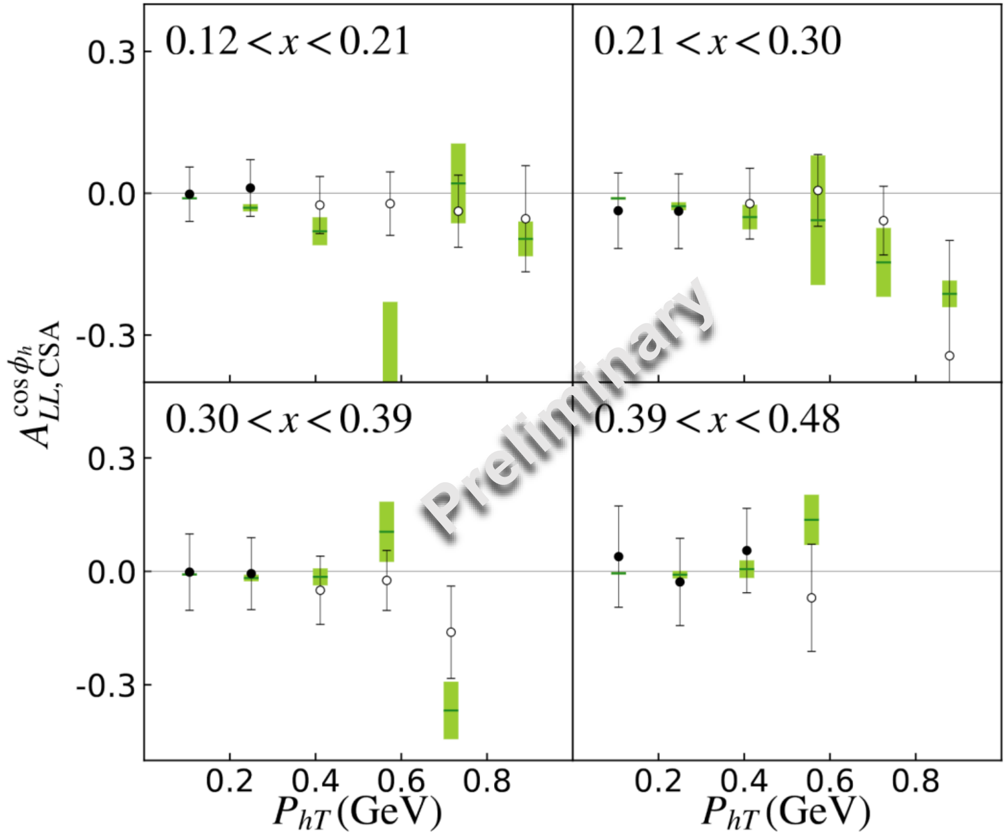

Backup——Energy Evolution

Evolution equation:

$$\mu \frac{\mathrm{d}\mathcal{F}(x, b_T; \mu, \zeta)}{\mathrm{d}\mu} = \gamma_\mu(\mu, \zeta)\mathcal{F}(x, b_T; \mu, \zeta)$$

$$\zeta \frac{\mathrm{d}\mathcal{F}(x, b_T; \mu, \zeta)}{\mathrm{d}\zeta} = -\mathcal{D}(\mu, b_T)\mathcal{F}(x, b_T; \mu, \zeta)$$

$$\Longrightarrow$$

$$-\zeta \frac{d\gamma_F(\mu, \zeta)}{d\zeta} = \mu \frac{d\mathcal{D}(\mu, b)}{d\mu} = \Gamma_{\text{cusp}}(\mu)$$

$$\gamma_F(\mu, \zeta) = \Gamma_{\text{cusp}}(\mu) \ln \frac{\mu^2}{\zeta} - \gamma_V(\mu)$$

$$F(x, b; \mu_f, \zeta_f) = \exp\left[\int_P \left(\gamma_F(\mu, \zeta)\frac{d\mu}{\mu} - \mathcal{D}(\mu, b)\frac{d\zeta}{\zeta}\right)\right] F(x, b; \mu_i, \zeta_i)$$

ζ-prescription:

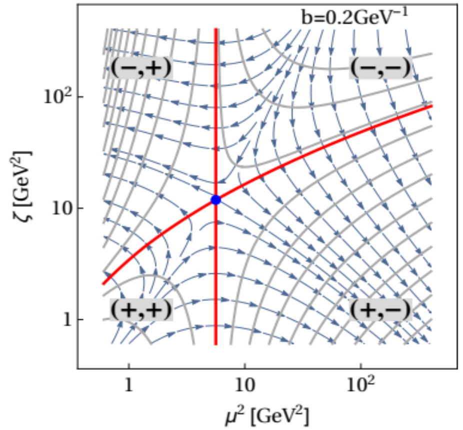

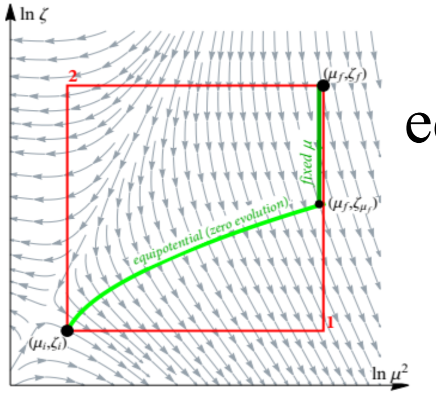

Saddle point: $\mathcal{D}(\mu_0, b) = 0, \quad \gamma_F(\mu_0, \zeta_\mu(\mu_0, b)) = 0$

equipotential lines: $$\frac{d \ln \zeta_\mu(\mu, b)}{d \ln \mu^2} = \frac{\gamma_F(\mu, \zeta_\mu(\mu, b))}{2\mathcal{D}(\mu, b)}$$

$$R[b_T; (\mu_i, \zeta_i) \to (Q, Q^2)] = \left[\frac{Q^2}{\zeta_\mu(Q, b_T)}\right]^{-\mathcal{D}(Q, b_T)}$$

Backup——χ^2 and Correlative Uncertainties

χ^2 form: $$\chi^2 = \sum_{\text{sets}} \sum_{i,j} (t_i - a_i)\, V_{ij}^{-1}\, (t_j - a_j)\,,$$

Covariance matrix: $$V_{ij} = \delta_{ij}\,(\sigma_i^{\text{uncor.}})^2 + \sigma_i^{\text{cor.}}\,\sigma_j^{\text{cor.}}\,,$$

Correlative uncertainties: $$\sigma_i^{\text{cor.}} = a t_i.$$

a is the overall correlative uncertainty factor comes from dilution factors and overall uncertainties of polarization of target and lepton beams.

Data set	Process	Target	Data points	polarization overall uncertainties	Dilution factor overall uncertainties
HERMES	$e^{\pm}p \to e^{\pm}hX$	H_2	160	6.6%	0
HERMES	$e^{\pm}d \to e^{\pm}hX$	D_2	317	5.7%	1.7%
CLAS	$e^{-}p \to e^{-}\pi^0 X$	$^{14}NH_3$	21	4.5%	5.8%
Total			498		

$$a = \sum_i \sqrt{a_i^2}$$

Backup——Parameters Results

World data fit:

Parameter	Value	Parameter	Value
N_u	$0.0223^{+0.0029}_{-0.0024}$	$N_{\bar{u}}$	$-0.008^{+0.092}_{-0.035}$
N_d	$0.0353^{+0.0051}_{-0.0088}$	$N_{\bar{d}}$	$0.006^{+0.032}_{-0.011}$
N_s	$-0.022^{+0.043}_{-0.043}$	N_g	$0.0220^{+0.0081}_{-0.0706}$
α_u	$2.78^{+0.45}_{-0.72}$	α_d	$4.28^{+0.38}_{-0.76}$
β_u	$0.145^{+0.041}_{-0.194}$	β_d	$1.16^{+0.14}_{-0.40}$
ϵ_u	$7.4^{+2.3}_{-4.5}$	ϵ_d	$-0.59^{+0.18}_{-0.20}$
λ_1	$0.240^{+0.062}_{-0.134}$	λ_2	$0.39^{+0.13}_{-0.33}$
λ_3	$0.92^{+12.17}_{-0.92}$	λ_4	$7.50^{+2.29}_{-0.78}$
λ_5	$-1.11^{+0.87}_{-0.50}$		

Backup——Parameters Correlation

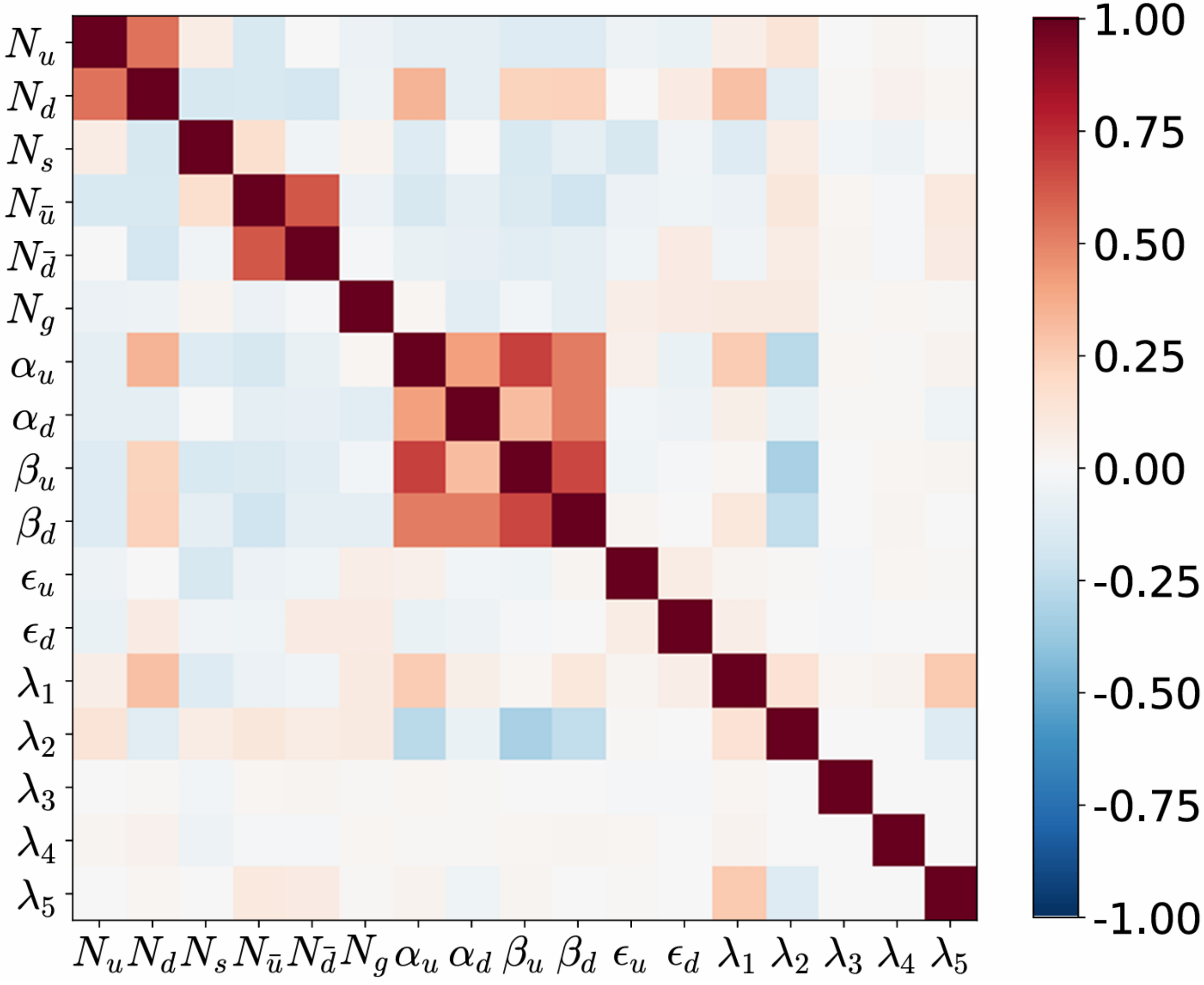

Backup——Positivity Bound

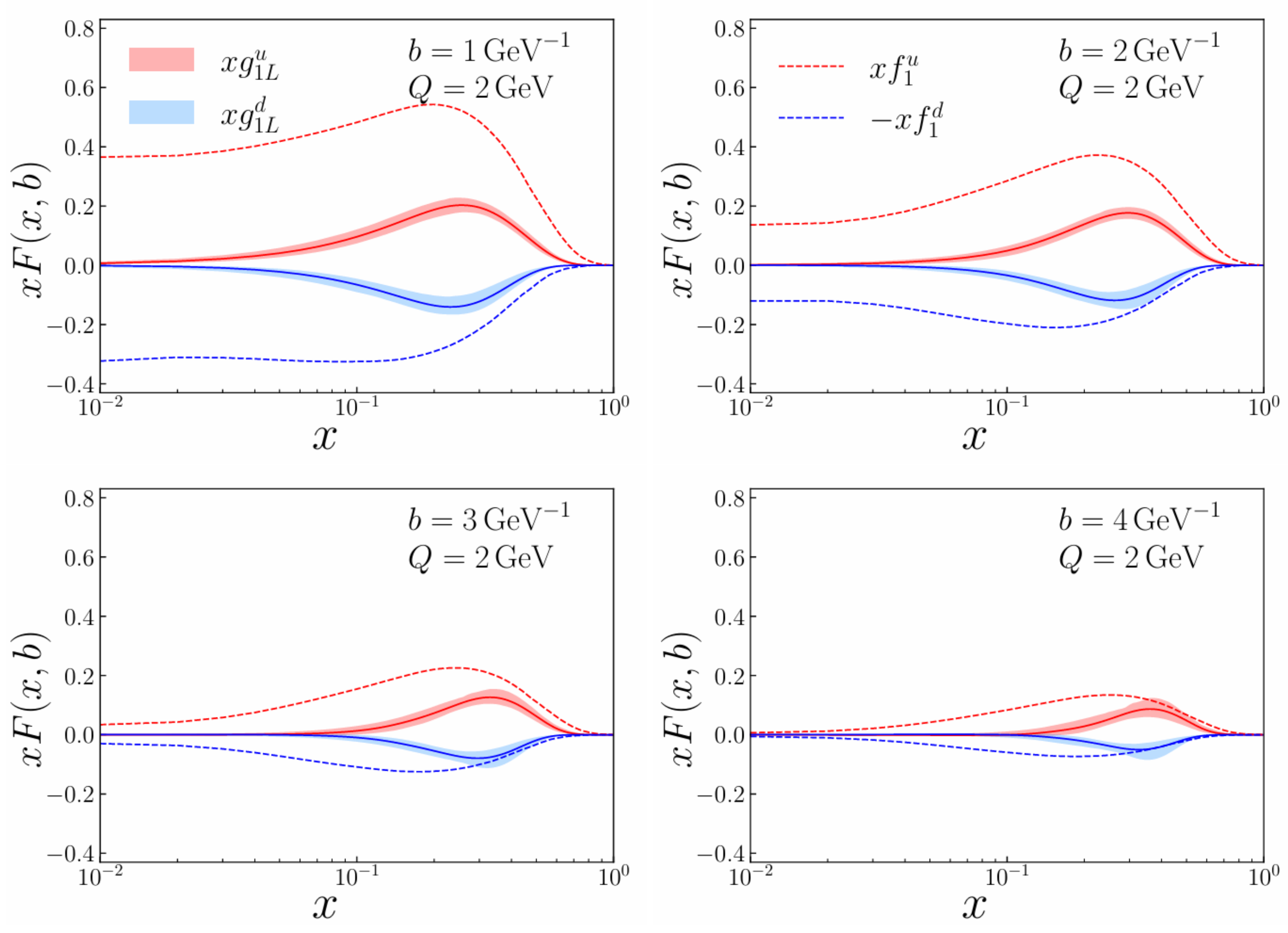

Positivity bound:
$|g_{1L}(x,k_T)| < f_1(x,k_T)$.

The positivity bound comes from probabilistic interpretation of parton distribution, however, *should not* be imposed during fitting procedure, which will result in results with bias.

We examine our result and no bound breaking is observed with the consideration of uncertainties.

Backup——Positivity Bound: Toy Model Test

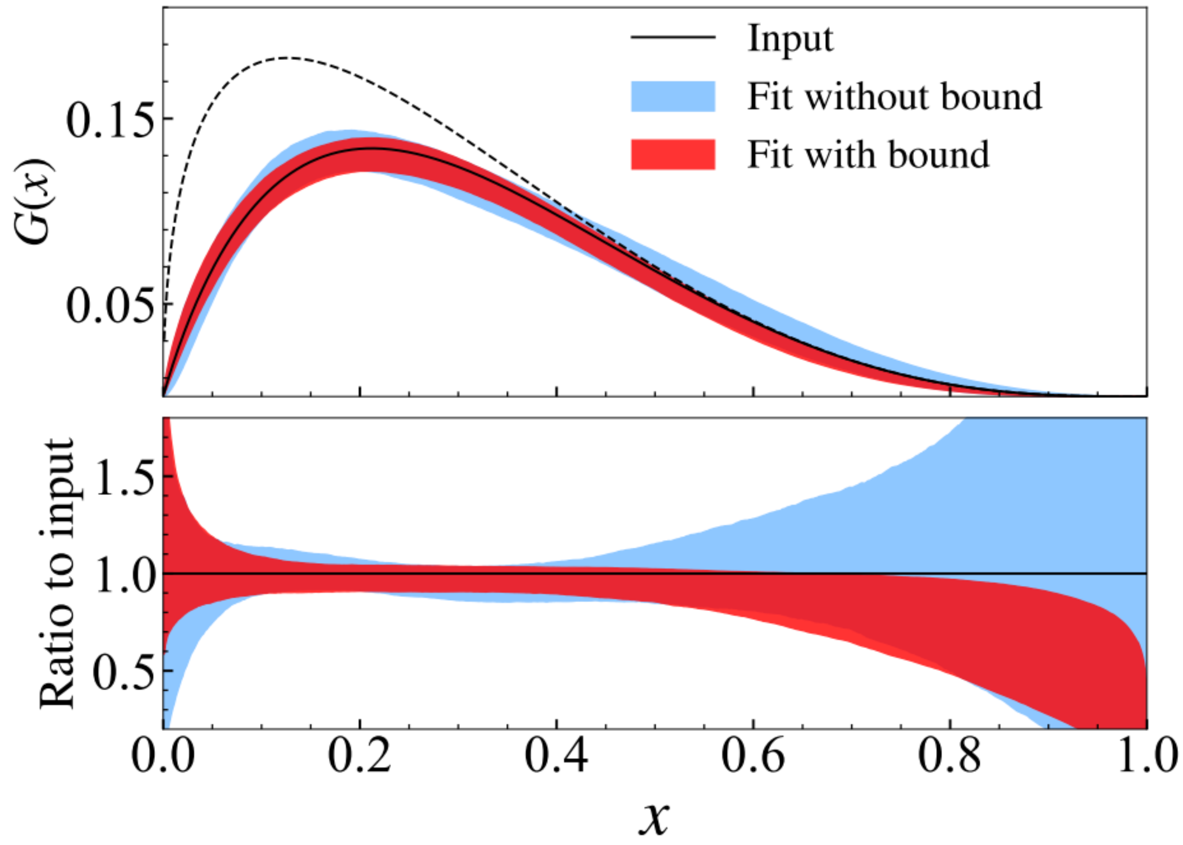

Toy model set:

$$F(x) = x^{0.5}(1-x)^3(1-\sqrt{x}+x),$$

$$G(x) = 2x(1-x)^3(1-\sqrt{x}+0.5x),$$

$$G(x) < F(x)$$

We generate asymmetry $G(x)/F(x)$ in 15 bins as pseudo-data, with a background disturbance $B(x)$. We compare the extracted $G(x)$ from the pseudo-data with and without the application of the positive constraint.

It was found that imposing the bound during the fitting procedure introduced a bias.

Backup——Fit with Fixed x dependent

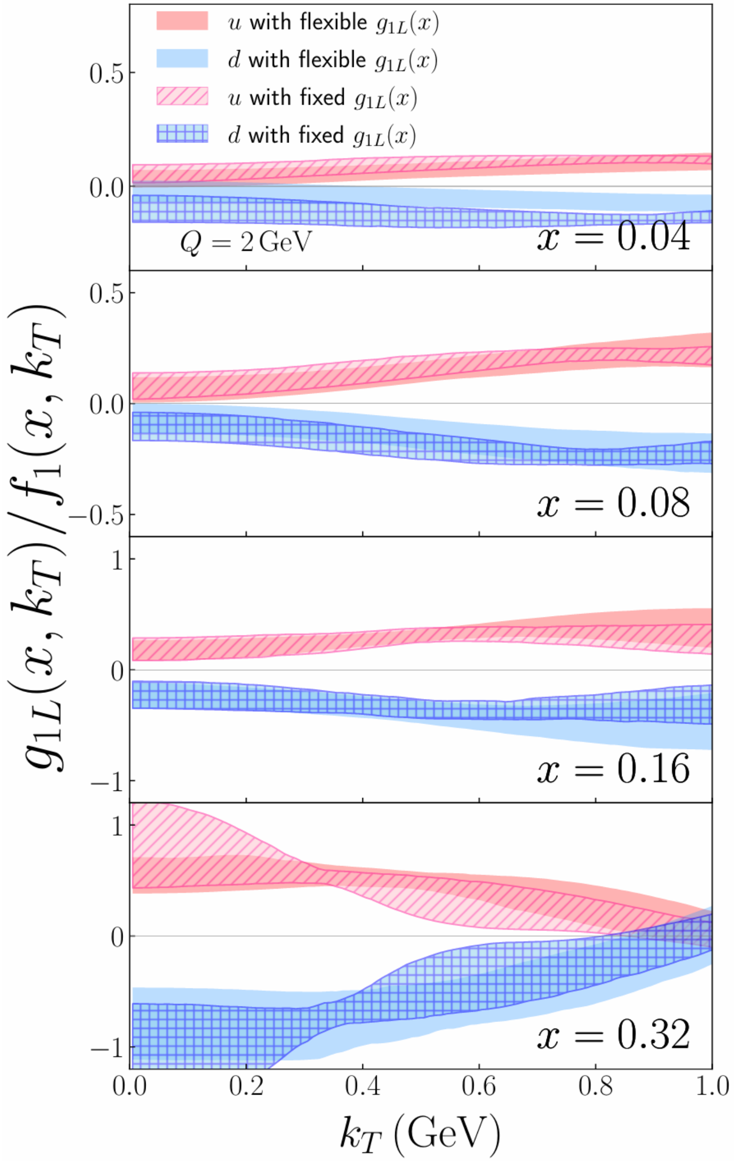

The collinear helicity distribution input with x-shape modification:

$$g_{1L}^{f}(x, \mu_{\mathrm{OPE}}) = N_f \frac{(1-x)^{\alpha_f} x^{\beta_f} (1+\varepsilon_f x)}{n(\alpha_f, \beta_f, \varepsilon_f)} g_1^f(x, \mu_{\mathrm{OPE}})$$

By setting $\boldsymbol{\alpha}, \boldsymbol{\beta}, \boldsymbol{\varepsilon} = 0$, one can remove x-shape modification.

The results show consistency within current uncertainties.

Backup——Fit with variation of TMD FFs

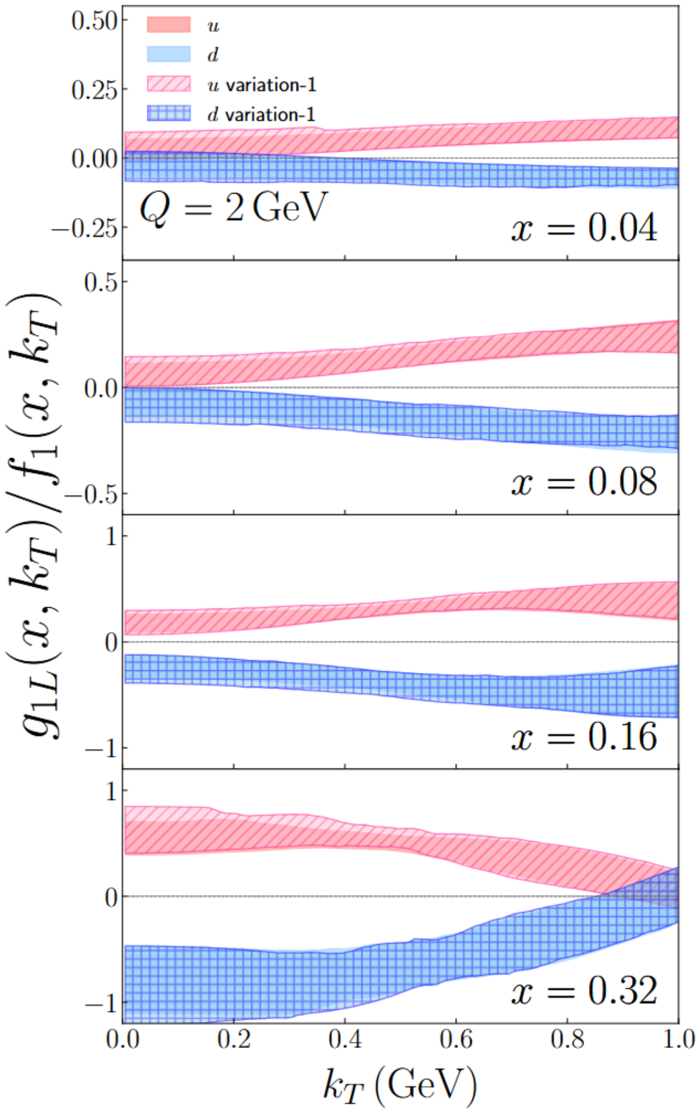

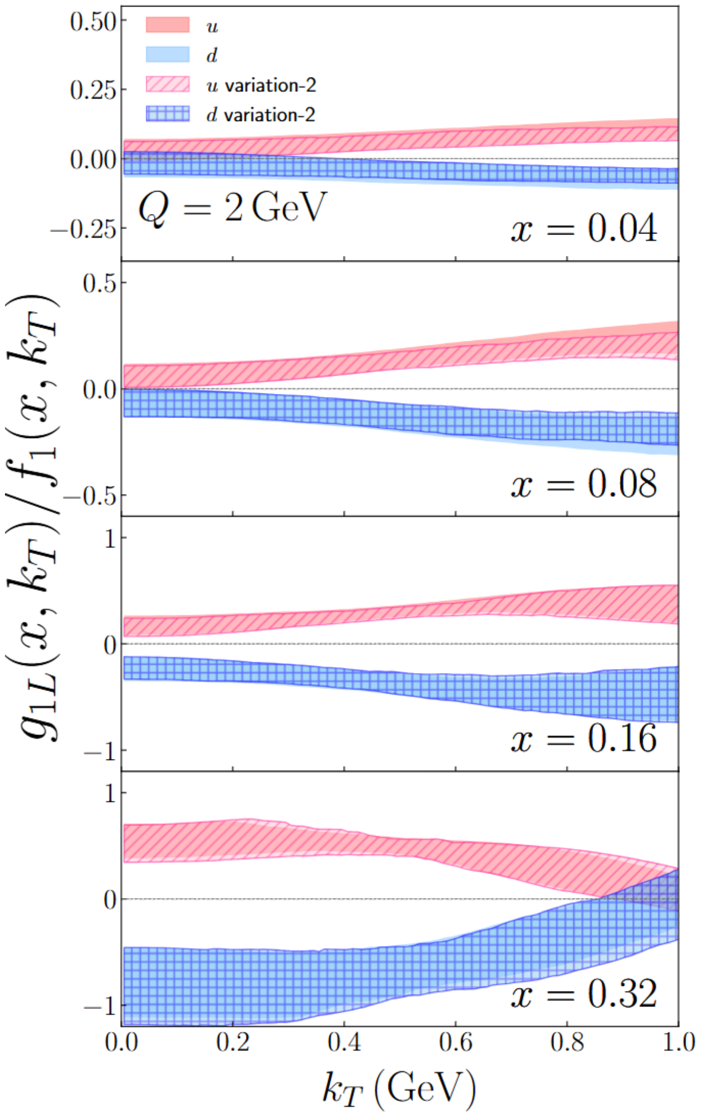

We vary the DSS FF input to a larger value as variation 1 and to a smaller value as variation 2.

It turns out that the quark polarizations

$$\frac{g_{1L}\left(x,k_T^2\right)}{f_1\left(x,k_T^2\right)} = \frac{q_{\uparrow}\left(x,k_T^2\right) - q_{\downarrow}\left(x,k_T^2\right)}{q_{\uparrow}\left(x,k_T^2\right) + q_{\downarrow}\left(x,k_T^2\right)}$$

are *not sensitive* to the FF input.